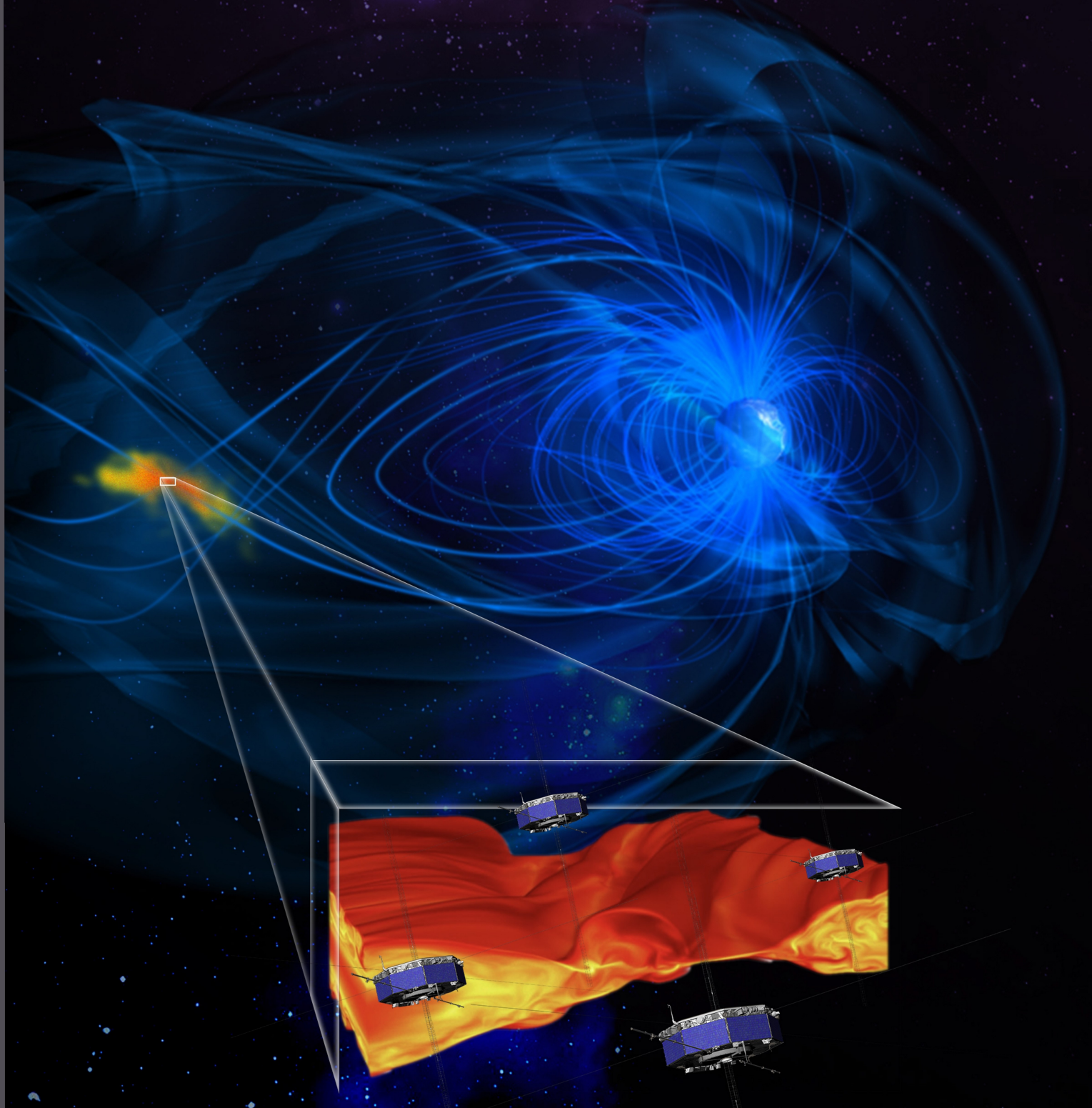


Magnetospheric Multiscale Mission (MMS): Extended Mission

B. L. Giles, MMS Project Scientist • J. L. Burch, MMS Science PI



Submitted to the 2020 Senior Review of the Mission Operations
and Data Analysis Program for Heliophysics Operating Missions
May 6, 2020

Table of Contents

1 Executive Summary	1
2 MMS Scientific Accomplishments	2
2.1 Investigate magnetic reconnection in the near-Earth space environment	2
2.2 Investigate the microphysics of collisionless shocks	4
2.3 Study the way turbulent processes interact on kinetic scales	5
2.4 Wave and particle dynamics in the magnetosphere	5
2.5 Heliophysics System Observatory (HSO) Science	5
3 Scientific Goals and Objectives for New Funding Period	5
3.1 Magnetic reconnection	6
3.2 Shock physics	10
3.3 Kinetic turbulence	11
3.4 Kinetic structures shaping the magnetospheric flank	13
3.5 Kinetic structures in the magnetosphere	14
3.6 Particle acceleration	16
4 Relation to NASA's Strategic Plan	19
4.1 Relevance to NASA's Heliophysics Strategic Goals	19
4.2 Role in the Heliophysics System Observatory	20
5 Implementation	21
5.1 Orbit and Campaigns	21
5.2 Configuration	21
5.3 Coordination with other missions in the HSO	22
5.4 Instrument modes	22
6 Technical Section: Mission Status	23
6.1 Instrument performance	23
6.2 Instrument status	23
6.3 Spacecraft system status	25
6.4 Mission operations status	25
6.5 Publications	26
6.6 Communication and public outreach	26
6.7 Succession planning, training, and diversity	26
7 Data and Code Management	27
8 Budget Justification	29
9 References	30
Appendix A: Acronym List	A-1
Appendix B: Code 300 Evaluation of End of Mission Plan	B-1
Appendix C: Budgets, Guideline and Overguide	C-1

1 Executive Summary

MMS has the overall objective of solving magnetic reconnection in the boundary regions of the Earth's magnetosphere. During the prime and first extended missions, we have discovered (1) the sources of the reconnection electric field and out-of-plane current for both asymmetric (dayside magnetopause) and symmetric (tail) reconnection, (2) the reconnection rate and the locations of energy conversion within the electron diffusion region (EDR), (3) the effects of a guide field and turbulence on reconnection physics, (4) generation of waves (lower hybrid, whistler, upper hybrid, Langmuir, Bernstein) by beam-plasma interactions and density gradients near and within the EDR and separatrixes, (5) the unexpected occurrence of reconnection within FTE's, Kelvin-Helmholtz vortices, the bow shock and dipolarization fronts, (6) electron-only reconnection in the turbulent magnetosheath, (7) acceleration of electrons to 100s of keV by turbulent parallel electric fields surrounding a tail reconnection event, (8) cold-ion effects on reconnection, and (9) the kinetic physics associated with interplanetary shocks, hot flow anomalies, and shock-produced plasma thermalization and ion acceleration. These results have been reported in over 500 papers in the refereed literature.

During the second extended mission MMS has three Science Goals:

- Understand how reconnection works in all boundary regions in Geospace.
- Understand particle acceleration processes in the outer magnetosphere and bow shock and their possible relationship to magnetic reconnection.
- Determine the nature of kinetic-scale turbulence and its role in reconnection and particle acceleration.

MMS is uniquely suited to accomplish these goals with its four-point measurements of particle and field measurements at the highest time resolution and accuracy ever achieved in space. During the senior review period MMS science is conducted in a set of campaigns (A–D) with emphasis on certain regions of space: A, duskside flank; B, dayside; C, dawnside flank; and D, magnetotail (Fig. 1.1).

In the first 3 years, during campaign B, the spacecraft explore the magnetopause at increasingly higher southern latitudes. This exploration culminates in 2023 with encounters of the southern magnetospheric cusp after which the apogee returns to

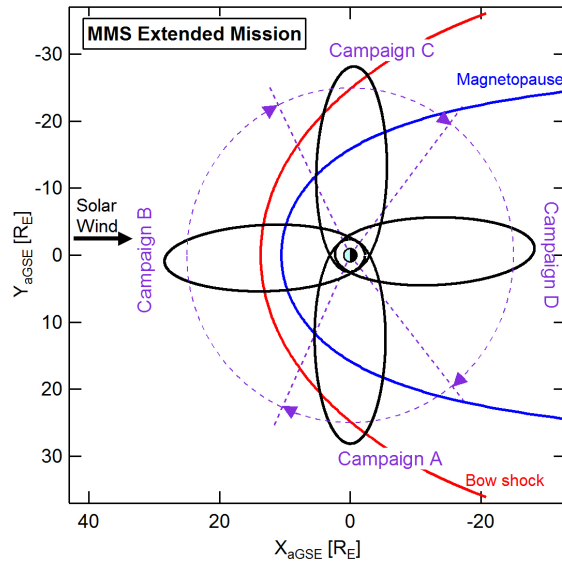


Fig. 1.1: MMS orbits divide into 5 campaigns with specific science focus based on the spacecraft location.

near the ecliptic plane by 2025. The MMS spacecraft remain in the tetrahedron configuration for the first three years. After 2023, there are changes to the spacecraft configuration. To minimize science disruption, these changes occur over days to weeks with minimal orbit maneuvers. One configuration that provides new science opportunities is a logarithmic string-of-pearls with separations approximating a geometric series, e.g., 30 km, 650 km, 15,000 km in order to sample electron, ion and MHD scales simultaneously.

Throughout the MMS mission there has been close coordination between the instrument teams and the theory and modeling (T&M) team. Early on, the MMS measurements confirmed several pre-flight predictions, including the displacement of the electron stagnation region from the X line on the day side and the crescent-shaped electron distributions that appear when reconnection is active. Later on, the T&M team has explained several MMS discoveries by employing 3D simulations with orders of magnitude more electrons. These discoveries included localized intense energy conversion, guide-field effects on reconnection, and turbulent particle acceleration.

Selection of burst-mode data intervals is made by an on-board system that looks for features in the burst data supplemented by the Scientist-in-the-Loop (SITL), who can view lower-resolution fast survey data. The SITL system is critical in that it

captures the majority of the burst intervals. To improve efficiency we have developed machine learning tools both for the on-board system and for the ground-based system, and these are very helpful to the SITL and may eventually replace the SITL. The only expendable on the spacecraft is hydrazine. There is about 30% left in the fuel tanks, which is enough to maintain tetrahedrons for 25+ years. This excess fuel also allows some maneuvers to other science-focused configurations.

In addition to the in-guide cost estimate there is an over-guide estimate. With the over-guide estimate the complete science objectives can be accomplished, whereas the in-guide cost will require severe prioritization with the result that only the primary mission objective of reconnection physics can be addressed. Objectives relating to turbulence, shocks, particle acceleration, and other important phenomena will have to be severely curtailed.

2 MMS Scientific Accomplishments

Over the 3 years since the last Senior Review, MMS made significant advances in the understanding of reconnection, shock, and turbulence physics, with over 400 papers published, including three *Science Reports* and two *Nature Letters*. This section highlights the MMS discoveries, many made in conjunction with other Heliophysics spacecraft. Table 2.1 shows that MMS has addressed all four proposed Prioritized Science Goals (PSGs) of the 2017 SR proposal, in addition to a number of new science topics.

2.1 Investigate magnetic reconnection in the near-Earth space environment

2.1.1 Symmetric reconnection in the magnetotail. MMS investigation of magnetotail reconnection revealed for the first time the key electron microphysics that enables reconnection in symmetric reconnection. The structure and dynamics of the symmetric electron diffusion region (EDR) was discovered to be profoundly different in many respects

from dayside asymmetric reconnection. Torbert et al. (2018) reported a textbook magnetotail electron diffusion region (EDR) encountered by MMS on July 11, 2017 (Fig. 2.1). The electron-scale plasma measurements revealed (a) super-Alfvénic electron jets reaching 15,000 km/s, (b) electron meandering motion and acceleration by the electric field, producing multiple crescent-shaped structures in the velocity distributions, (c) spatial dimensions of the electron diffusion region consistent with a reconnection rate of ~0.1-0.2. Furthermore, Nakamura, R. et al. (2019) demonstrated that the frozen-in condition within the EDR was broken by non-gyrotropic pressure and inertial forces associated with the crescent electrons, and the EDR dimension was related to the gyro-scale of trapped electrons. The well-structured multiple layers of electron populations indicate that, despite the presence of turbulence near the reconnection site, the key electron dynamics in the EDR appears, remarkably, to be largely laminar.

2.1.2 Acceleration of electrons to high energies by turbulent parallel electric fields surrounding tail reconnection. Ergun et al. (2018) reported acceleration of electrons to a few hundred keV in a region surrounding a tail reconnection site. It was shown for the first time that turbulent parallel electric fields with amplitudes >100 mV/m are associated with these high-energy electrons with $\mathbf{J} \cdot \mathbf{E}_{\text{par}}$ accounting for as much as 20% of the total energy conversion. These results give insight into the long-standing mystery of substorm-related particles with energies far above what can be accounted for by reconnection electric-fields alone.

2.1.3 Asymmetric reconnection at the magnetopause. MMS continues to provide crucial measurements of the electron-scale kinetic physics of asymmetric reconnection. Webster et al. (2018) used established characteristics of EDRs to identify 21 magnetopause EDRs in MMS Phase One data alone. These events revealed the persistent presence of turbulent Ohmic energy exchange on the magnetosphere side of the X-line. The dominant non-

Table 2.1: Accomplishments of 2017 SR Prioritized Science Goals (PSG) and Sub-Goals, and beyond.

PSG1: Investigate magnetic reconnection in the near-Earth space environment	§2.1.1, 2.1.2, 2.1.3, 2.2
PSG2: Study the processes that heat plasma and accelerate particles to large energies	§2.1.2, 2.1.7, 2.2, 2.5
PSG3: Study the way turbulent processes interact on kinetic scales	§2.3, 2.1.2., 2.1.8
PSG4: Investigate the microphysics of collisionless shocks	§2.2, 2.1.8
Additional Science and Discoveries	§2.1.4, 2.1.5, 2.1.6, 2.1.7, 2.1.8, 2.2, 2.3, 2.4., 2.5

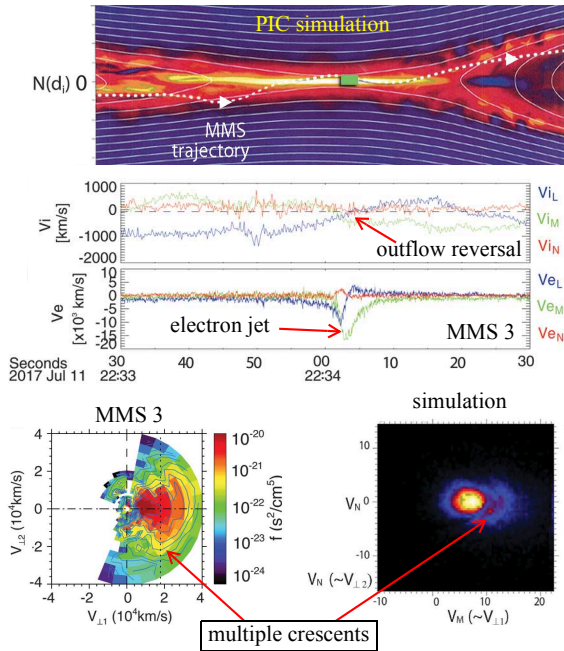


Fig. 2.1. MMS encounter of a textbook electron diffusion region in the magnetotail, detecting super-Alfvénic electron jets and multiple-crescent electron distributions (Torbert et al., 2018).

ideal term in the diffusion regions was found to be the electron pressure tensor divergence, which was a factor of ~ 5 larger than the electron inertia term (Genestreti et al., 2018).

Although 2D simulations of reconnection show a quasi-laminar transfer of magnetic flux into particle energization, MMS revealed the common occurrence of electron-scale islands of alternating energy exchanges, with amplitudes two orders of magnitude larger than expected (Burch et al., 2018a). 3D simulations have closely reproduced these features (Swisdak et al., 2018), and found that the islands are related to the alternating annihilation and generation of highly-localized pockets of fluctuating out-of-plane Hall magnetic fields.

2.1.4 Guide field effects. MMS has revealed that the out-of-plane (guide) magnetic field can affect the structure and dynamics of reconnection in a significant way. In strong guide field reconnection, the parallel electric field is strongly enhanced, and the energy conversion is dominated by parallel electric fields and field-aligned currents (Wilder et al., 2018), as opposed to dominantly perpendicular dissipation in antiparallel (weak guide field) reconnection. In several guide field events, the observed parallel electric field was found to be an order of

magnitude larger than predicted by theory and 2D simulations, implying 3D and/or transient effects (Fox et al., 2018). In the reconnection exhausts, the presence of even a moderate guide field can lead to significant asymmetries in the spatial structure of the parallel electric field, leading to asymmetric heating and acceleration of the ions and electrons (Eastwood et al., 2018). The latter suggests that particles are energized differently with and without guide fields.

2.1.5 Cold ion effects. Cold ions of ionospheric origin often dominate the mass density of the Earth’s outer magnetosphere. MMS revealed how these cold ions are accelerated and heated via wave-particle interactions (Toledo-Redondo et al., 2018), and the effect is amplified when the ionospheric outflows include heavy ions such as O^+ (Fuselier et al., 2019).

2.1.6. Wave effects. MMS has made important contributions to the understanding of the generation of plasma waves and their roles in anomalous particle transport in reconnection. Nongyrotropic electron crescent distributions generated in EDRs were found to be unstable and produced large-amplitude upper hybrid and Langmuir waves (Graham et al., 2018; Burch et al., 2019). Kinetic simulations showed that the waves can undergo nonlinear processes, resulting in the generation of radio waves and electrostatic harmonics (Dokgo et al., 2019). MMS also detected whistler waves generated by electron temperature anisotropy and electron beams in EDRs (Burch et al., 2018b). At lower-frequencies MMS detected lower hybrid drift waves generated by the interaction between magnetosheath ions penetrating into the magnetosphere with magnetospheric ions (Graham et al., 2019). These waves could lead to the previously unexplained cross-magnetic-field plasma diffusion across the magnetopause. This effect was subsequently shown to occur in 3D simulation systems, but not in 2D models owing to the suppression of wave modes in 2D (Le et al., 2018). Finally, electromagnetic drift waves were detected at the magnetopause and found to be coupled to higher-frequency parallel electric fields, suggesting that they may cause secondary reconnection (Ergun et al., 2017).

2.1.7 Magnetic flux rope dynamics. Magnetic flux ropes play an important role in the transport of energy throughout the Sun-Earth system. At the magnetopause, MMS observed reconnection in compressed current sheets at the interface between colliding magnetic field lines originating from two

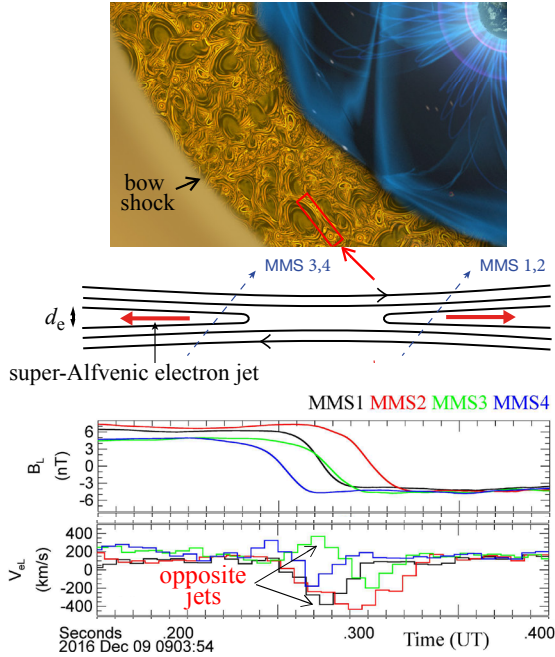


Fig. 2.2: MMS discovery of electron-only reconnection (without ion coupling) in turbulent plasmas downstream of quasi-parallel bow shock (Phan et al., 2018).

reconnection X-lines (Øieroset et al., 2019).

In the magnetotail, kinetic-scale flux ropes were observed downstream of EDRs containing large-amplitude parallel electric fields and particle acceleration (Stawarz et al., 2019). Marshall et al. (2019) reported evidence for reconnection and electron heating inside a flux rope embedded within the front of magnetotail reconnection jets.

2.1.8 Electron-only reconnection in the quasi-parallel bow shock and magnetosheath. The specially produced ultra-high (7.5 ms) resolution electron measurements led to the surprising discovery of a new mode of reconnection involving only electrons, detected in the turbulent magnetosheath (Phan et al., 2018) (Fig. 2.2), and within the bow shock transition region (Gingell et al., 2019; Wang et al., 2019). The absence of ion coupling is likely due to insufficient space and/or time for the ions to couple to the small-scale magnetic structures in turbulence.

2.2 Investigate the microphysics of collisionless shocks

The capabilities of MMS have enabled several landmark studies in shock physics. The discovery of magnetic reconnection within the shock layer suggests that reconnection disentangles the turbulent

shock fields and contributes to the overall shock heating (Gingell et al., 2019). In terms of the more traditional shock heating mechanisms, MMS demonstrated the role of high and low-frequency whistler waves in scattering electrons at the shock fronts, a necessary ingredient for the acceleration of electrons to high energies (Oka et al., 2019). MMS also found evidence for the autogenous acceleration to MeV energies of ions trapped between large transients in the foreshock and the main bow shock (Fig. 2.3) (Turner et al., 2018). Other important studies of particle “thermalization” in shocks include the discovery of ripples propagating along the shock front (Johlander et al., 2018), which can magnetically trap electrons rendering magnetic pumping an efficient heating mechanism (Lichko et al., 2020).

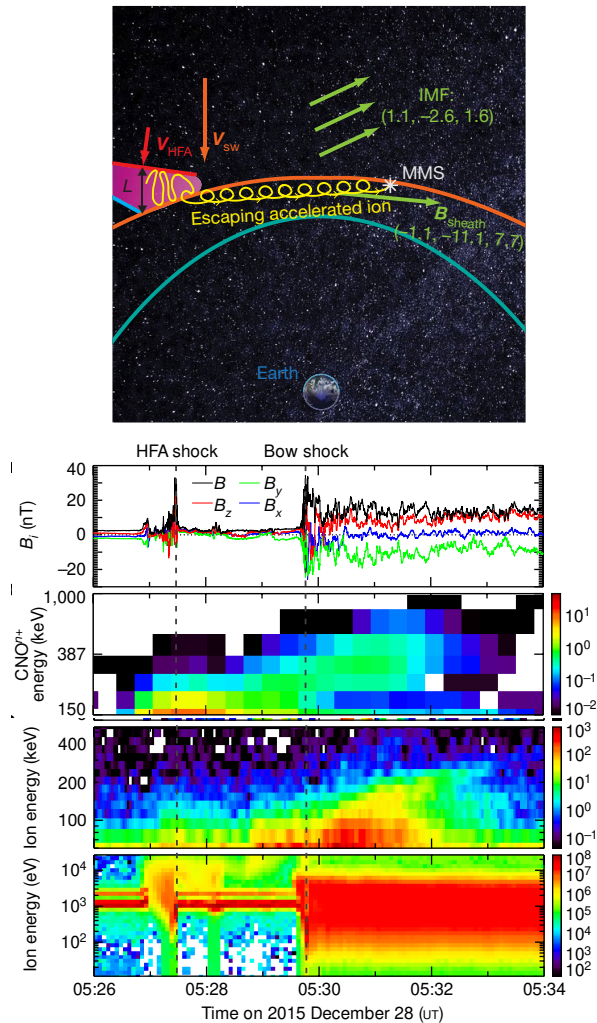


Fig. 2.3: MMS discovery of first-order Fermi acceleration up to MeV energy of ions trapped between a hot flow anomaly and the bow shock (Turner et al., 2018).

2.3 Study the way turbulent processes interact on kinetic scales

The marriage of single point and multipoint measurements at kinetic scales allowed Chasapis et al. (2017) to directly compare correlation and spectral measurement of second order (spectra) and fourth order statistics in both the solar wind and the magnetosheath. Innovative studies included studies of sub-ion scale cascade quantities (Breuillard et al., 2018) and simultaneous measurements of energy cascade rates at three scales (Bandyopadhyay et al., 2018). Intermittency of current sheets and electromagnetic work on particles in magnetosheath turbulence were studied using unique capabilities of MMS to measure pressure tensors and velocity gradients (Chasapis et al., 2018).

2.4 Wave and particle dynamics in the magnetosphere

MMS high time resolution ion composition and field measurements have allowed for in-depth investigations of electromagnetic ion cyclotron (EMIC) wave properties and wave-particle interactions. Kitamura et al. (2018) demonstrated for the first time direct energy transfer from the local hot proton population in the outer magnetosphere to EMIC waves through the cyclotron resonance, and from EMIC waves to cold He^+ ions via non-resonant interaction. Through observations of the wave Poynting vector and ion populations, Vines et al. (2019) was able to identify the free energy source of the EMIC waves and pinpointed an off-equator source region.

In the inner magnetosphere, Cohen et al. (2019) discovered a drift-dispersed energetic electron signature that sheds new light on particle injection processes.

2.5 Heliophysics System Observatory (HSO) Science

MMS has been employed alongside a variety of

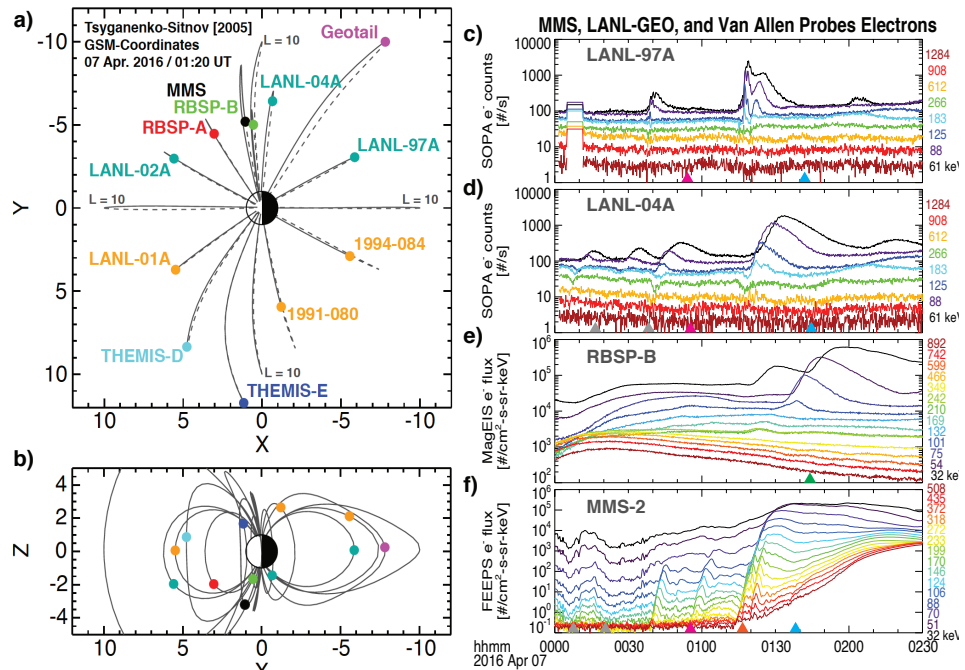


Fig. 2.4: Multiple HSO observations showing the propagation of an energetic electron injection throughout the inner magnetosphere (Turner et al., 2017).

other spacecraft in the HSO to develop a clearer picture of how the magnetosphere and its various plasma regimes respond to different driving conditions. Turner et al. (2017) used 15 spacecraft throughout the plasma sheet and inner magnetosphere to study substorm activity and associated energetic particle injections, finding that our best conceptual models are unable to explain all features observed during multiple events throughout the system (Fig. 2.4). Engebretson et al. (2018) examined EMIC wave activity throughout the inner magnetosphere associated with an interplanetary shock impact using data from MMS, VAP, GOES, and four ground magnetometer stations. Wave-particle interactions between large-amplitude Pc5 ULF waves and 10s of keV protons and oxygen ions were examined using a combination of MMS and Arase data by Oimatsu et al. (2018), who found that both drift and bounce resonances were active. Lu et al. (2019) compared KH waves observed simultaneously by MMS and THEMIS and found that the wave activity was quasi-symmetric on both dawn and dusk flanks.

3 Scientific Goals and Objectives for New Funding Period

MMS remains our unique access to high precision and high-cadence particle and field measure-

ments, far beyond what any other mission could provide previously. MMS overall scientific goals are in line with NASA’s overall goals for Heliophysics research. They are 1. *Understand how reconnection works in all boundary regions in Geospace*, 2. *Understand particle acceleration processes in the outer magnetosphere and bow shock and their possible relationship to magnetic reconnection*. 3. *Determine the nature of kinetic-scale turbulence and its role in reconnection and particle acceleration*. Our proposed science objectives are designed to solve the most prominent scientific questions within these overarching goals. They are also chosen to take advantage of this unique research opportunity by emphasizing microphysics research in a variety of contexts of great import to space plasma physics and magnetospheric physics. In addition, and particularly for the later phases of the mission, we outline a progressive research plan, which increasingly includes research objectives on larger spatial scales.

Table 3.1 shows the science objectives and their relationship to the in-guide and over-guide budgets. In the over-guide budget, all science objectives are achieved. In the over-guide budget, tetrahedron configurations are used for the first 3 years of the senior review period and then string-of-pearls and other novel configurations are used to investigate cross-scale physics. In the in-guide budget, selected sub-objectives in three main areas are achieved and spacecraft configurations are limited to tetrahedrons at electron and ion scales.

3.1 Magnetic reconnection

As appropriate for the unique opportunity MMS provides to understand magnetic reconnection, this

topic remains one of the main foci of the extended mission. Broadly seen, reconnection research has two emphases: verify our understanding of how reconnection works on the electron scale, and extend reconnection research to ion scales, large scale energy transfer, and to more complex dynamical situations. The former emphasis is addressed whenever MMS encounters an electron diffusion region. New and substantial extensions of reconnection research, based on the uniquely powerful combination of measurements and accompanying theory and modeling, are described in the following sections.

3.1.1 How are kinetic scales and fluid scales connected in magnetopause reconnection? Magnetic reconnection is an intricate interplay of processes on large and small scales. Large-scale processes determine the overall reconnection inflow or driving rates, and kinetic scales determine details of the energy conversion and dissipation. With MMS we have made tremendous progress understanding the EDR. However, how exactly energy conversion occurs on scales larger than those of the electrons, and how the kinetic physics both adjusts to and feeds back on the larger scale inflow, remain open questions. Key issues must be resolved, such as whether fluctuations in magnetic reconnection can be driven by rapid time changes or substantial shear flows in the inflow region and how reconnection behaves when heavy ions become entrained in the inflow. Study of these processes is critical for the development of a complete understanding of reconnection and the resulting energy input into the magnetosphere.

3.1.1.1 How does reconnection convert energy and how are electrons heated? Fundamental questions remain regarding the coupling of the multi-scale pro-

Table 3.1: Science Objectives and their achievability within budget constraints. All SO’s achieved in over-guide budget.

Science Objectives	Science Objectives Achieved in Over-Guide Budget	SO’s achieved in In-Guide Budget
3.1 Magnetic Reconnection	3.1.1, Connecting Kinetic and Fluid Scales; 3.1.2 Instabilities and Energy Conversion in the Magnetotail in tetrahedron and special configurations	3.1.1, 3.1.2 only in tetrahedron configuration
3.2 Shock Physics	3.2.1 Bow shock; 3.2.2 Interplanetary Shocks, in tetrahedron and special configurations	None
3.3 Kinetic Turbulence	3.3.1 Evolution of Magnetosheath Turbulence; 3.3.2 Large-scale turbulence properties	3.3.1 only
3.4 Kinetic Structures at the Magnetospheric Flanks	3.4.1 Kinetic structure of KH vortices;	None
3.5 Kinetic Structures in the Magnetosphere	3.5.1 Wave-particle interactions at dipolarization fronts; 3.5.2 Kinetic structure in the plasma sheet boundary layer; 3.5.3 Thin flapping current sheets	None
3.6 Particle Acceleration	3.6.1 Scale sizes of EMIC and ULF waves; 3.6.2 Earth’s Radiation belt electrons; 3.6.3 Species dependent ion acceleration in the magnetotail; 3.6.4 Physics of the magnetospheric cusps	3.6.4 only

cesses that comprise dissipation of magnetic energy during reconnection, including a complete view of the role whistler waves play in reconnection. For instance: (i) are ion or fluid-scale features of reconnection (e.g., the reconnection rate) affected when turbulent, wave-driven, or laminar modes drive electron dissipation in the EDR? (ii) How do non-gyrotropic electron distributions thermalize? (iii) How are magnetosheath electrons and ions heated by magnetic reconnection? (iv) What is the link between whistler waves in the EDR, the flux pile-up region, and the separatrices?

3.1.1.2 How do cold and heavy ions impact magnetic reconnection? The fact that cold populations at times persist for some distance into the reconnection exhaust without being isotropized and heated points to entry locations and interactions of the cold magnetospheric populations with the magnetopause and X-line that are spatially variable. Just how the populations evolve across the magnetopause separatrices and into the reconnection exhaust, and how those populations may affect or be affected by reconnection is still not understood, particularly for heavy ions present at the magnetopause (He^+ , He^{++} , O^+).

3.1.1.3 What is the impact of magnetosheath fluctuations on magnetopause reconnection? Observations of magnetopause reconnection often indicate the presence of fluctuations in all regions, from the diffusion region to the outflow region. A number of wave modes have been identified as possible internal causes for fluctuations away from the EDR. On the other hand, we expect that the turbulent magnetosheath, which forms one of the inflow regions for the reconnection process, will provide an external driver of fluctuations in the reconnecting layer. Among others, this view is supported by modeling results indicating that the orientation of the reconnection line depends on the magnetic field directions in the inflow regions. A rapid time variation of the magnetic field in the sheath-side inflow regions would then generate a rapid re-orientation of the reconnection diffusion region and consequently a large amount of turbulence. Other effects potentially translating into fluctuations in the reconnection layers are variations in magnetosheath pressure and flows. It is important to understand how reconnection works under fluctuating inflow conditions and, consequently, which of the observed fluctuations are internally or externally generated.

3.1.1.4 What are the effects of flow on low-latitude magnetopause reconnection? Flow shear across the magnetopause is common and may affect aspects of reconnection, e.g., the reconnection rate, the stability and motion of a reconnection site, the efficiency and mechanism for electron dissipation and demagnetization. However, the precise effects of flow shear on asymmetric magnetopause reconnection are not well understood. At low latitudes, the prevalent magnetosheath flow is primarily perpendicular to the magnetospheric magnetic field. For southward IMF, it is not known whether (i) stable low-latitude reconnection persists in the presence of a super-Alfvénic flow shear or reconnection in Kelvin-Helmholtz (KH) vortices dominates in this regime, (ii) the reconnection rate is reduced or suppressed by flow shear in the outflow direction larger than twice the Alfvén speed, and (iii) the electron pressure tensor-based EDR model is generally valid for a wide range of upstream conditions in the presence of a super-Alfvénic out-of-plane flow shear.

3.1.1.5 What are the effects of flow shear on high-latitude magnetopause reconnection? Reconnection at the high-latitude magnetopause provides the opportunity to study reconnection when magnetosheath flows are directed primarily parallel to the local geomagnetic field. This type of reconnection has been studied by the Polar and Cluster missions; however, investigations of the electron physics involved in this type of reconnection can only be conducted by MMS. The fact that MMS reaches this region through orbital precession provides a unique opportunity to understand how reconnection works under these conditions. Specific questions to be addressed are: (i) How does the reconnection process change in the presence of cold plasma streaming parallel or obliquely to the magnetic field? (ii) How do the electron-scale processes match this plasma inclusion, and how does the interaction between the larger scales and electron scales work under these conditions? and (iii) How is the electron diffusion region being “picked up” by the moving plasma and swept into the anti-sunward direction?

3.1.1.6 What are the generation mechanisms of flux transfer events? Flux transfer events (FTEs) are ubiquitous signatures of highly time-dependent reconnection. Nevertheless, their generation mechanisms remain under debate, as does the question of whether there is only one mechanism operating all

the time, or different ones at different times. Three models of FTEs have been proposed: The original one in which two isolated elbow-shaped flux ropes move north/south away from the reconnection line; the bursty single X-line model; and the multiple X-line model. The question of which model applies remains largely open. While the connection to an X-line rules out the original FTE model, we need to understand under what conditions do FTE signatures (such as magnetic connectedness, plasma flows, etc.) match the single or multiple X-line model. How can we explain the (occasional) reversals of ion flows along the separatrices? How do we explain the repeated co-existence of crater and normal FTEs on the same magnetopause crossing? Answers to these long-standing questions will reveal not only the origin of FTEs but also provide new information regarding the nature of time-dependent magnetopause reconnection.

Researching these topics with MMS. A holistic understanding of magnetic reconnection on multiple scales requires the simultaneous resolution of kinetic-scale diffusion regions and their fluid-scale boundary conditions, which only MMS can provide, as well as synergistic theory and modeling. MMS has successfully employed electron-scale measurements to determine, e.g., how the frozen-in condition is broken and how electrons are accelerated in the EDR. Determining the context and ramifications of these processes requires a new multi-scale configuration, one application of which is shown (Fig. 3.1 – see also §5). Simultaneous measurements are taken in four key areas: (1) MMS4 determines the magnetosheath boundary of the diffusion region some 60 km or $\sim 1 d_i$ upstream, (2) another S/C observes the acceleration of non-gyrotropic electron crescent distributions in the EDR, (3) a third S/C observes the formation of the super-Alfvénic electron jets some ≤ 20 km or $\sim 15 d_e$ downstream in the outflow, and (4) the final S/C observes the thermalization of the electrons, the final step in the electron dissipation process, some 60 km downstream. The conditions of the upstream magnetosphere, which typically provides the EDR with steady input, are determined before/after the EDR crossing, allowing for assessment of heavy and cold ions, shear flows, and jets in the inflow. For crossings not involving the EDR, the same configuration lends itself to the study of FTE structure as well as cold and heavy ion ener-

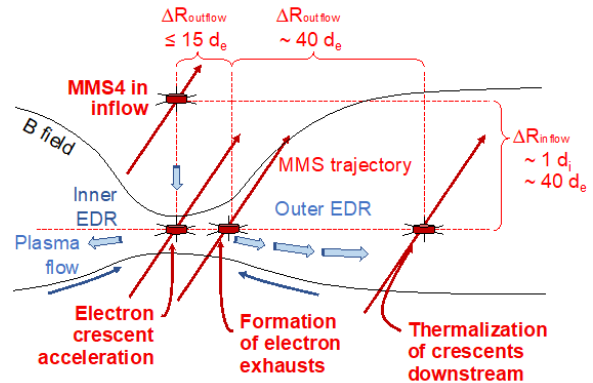


Fig. 3.1: Investigating cross-scale coupling of electron dissipation during magnetic reconnection by the simultaneous resolution of ion and electron-scale processes. As the magnetopause EDR moves across the irregular tetrahedron, the spacecraft resolve reconnection in the EDR, its upstream/downstream boundary conditions, and key aspects of the multi-scale electron dissipation process. Larger spacecraft separations can extend this type of research into fluid scales and the interface between the diffusion region and the more distant outflow.

gization in the outflow region. Knowledge gained from EDR observations by the electron-scale tetrahedron are used to classify signatures of instabilities, wave-particle interactions, energy conversion modes, etc. measured by single S/C, while a more widely spaced constellation is used to characterize cross-scale and cross-region coupling processes. In this way, MMS's unique capabilities will solve the multiscale properties of magnetic reconnection.

Extensions via the HSO. While the fluid-to-kinetic-scale MMS configuration studies the local physics of magnetopause reconnection, the system-scale constellation formed by MMS, Cluster, THEMIS, and Geotail can study the magnetopause and inflow regions at different local times and longitudes. MMS relates local (in time and space) upstream conditions with energy conversion and outflow acceleration processes, and the HSO determines the upstream conditions and outflow characteristics over the scale of the extended low-latitude reconnection site.

3.1.2 How do instabilities facilitate energy conversion in the magnetotail? The separatrices of magnetic reconnection are well known to extend long distances away from the reconnection diffusion region. The separatrix regions are kinetic scale surfaces, which bound the inflow and outflow regions. The separatrices are characterized by electrons ac-

celerated toward the X line forming beams, density gradients, cross-field currents, and velocity shears, all of which are potential sources of instability. The instabilities can result in a wide variety of waves developing in the separatrices of reconnection, including electrostatic solitary waves, whistler waves, lower hybrid waves, and Langmuir waves. Many of these waves have been reported in observations, but multi-spacecraft observations are required to determine the role of gradients and velocity shears as sources of instability. Plasma gradients and cross-field currents are known to produce lower hybrid waves in reconnection separatrices, and evidence of velocity shear instabilities has been reported in particle-in-cell simulations of magnetic reconnection.

Which instabilities are driven by velocity shears and plasma gradients at the separatrix? At the separatrices, velocity shears in the normal direction of the parallel flowing electrons and the cross-field (out-of-plane) both occur. These velocity shears, as well as plasma gradients, are potential sources of instability and may significantly modify other instabilities developing in reconnection separatrices. Velocity shears can generate lower hybrid-like waves or electron Kelvin-Helmholtz-like waves. The effect of velocity shear or that of gradients on the separatrices has not been comprehensively investigated with spacecraft observations. Hence, the overall importance of these processes to reconnection has not been established. Such processes can contribute to particle acceleration, mixing between different particle populations, particle transport, and broadening of the boundary. The science questions are then: what roles do velocity shear and plasma gradients play in generating waves, modifying the properties of waves, and modulating energy conversion processes in the separatrices of magnetotail reconnection, and, specifically, how are electrons energized at this boundary?

Researching these topics with MMS. To answer the above science questions requires the velocity shears in the separatrices to be measured and compared with other gradients and suitable

model results. The length scales of the waves are related to electron kinetic scales (tens to a hundred km). To characterize electrostatic waves and lower-hybrid waves two spacecraft need to be separated by a distance comparable to or below the length scales of the waves (20-30 km) both parallel and perpendicular to the magnetic field. To resolve plasma gradients on the order of a hundred kilometers, MMS needs to measure plasma moments at two locations separated by a distance of ~ 100 km in the direction normal to the separatrix. Figure 3.2 illustrates the proposed spacecraft configuration – one of the configurations discussed in §5. There is a possibility to have the spacecraft grouped in two pairs for equal wave measurements at two locations simultaneously, or as a trio and single spacecraft, similar to the configuration for magnetopause studies, to have more detailed wave measurements at one location. MMS will for the first time determine the role of key wave modes at the separatrix in the larger context.

Extensions via the Heliophysics Systems Observatory. The HSO can contribute to investigating the process of electron acceleration and heating at the separatrices by providing an even larger scale view of the reconnection region. For example, the apogee of Cluster is close to 0.65 that of MMS. At the inbound leg of the MMS orbit, when MMS investigates the electron and ion scale kinetic physics, Cluster (along its polar orbit) provides a good overview of the current sheet cross section (one to a few R_E) closer to the Earth.

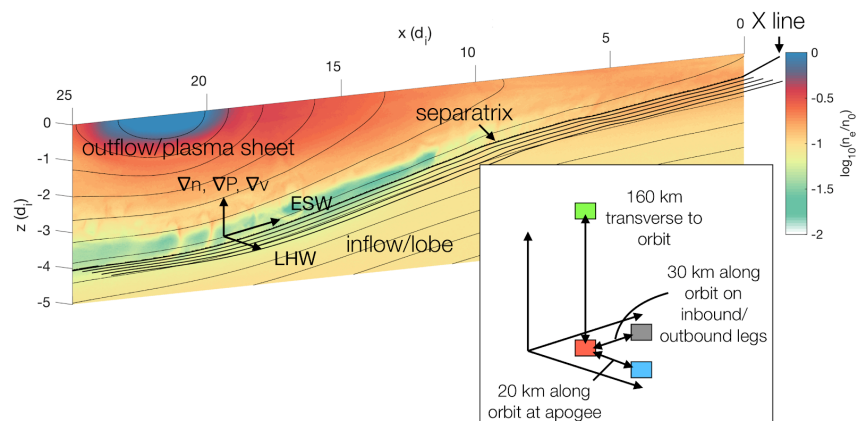


Fig. 3.2: Resolving the separatrix environment of symmetric reconnection. Plasma gradients are resolved by two spacecraft with a cross-orbit separation comparable to but below ion kinetic scales. ESW and LHW properties are measured by a minimum of two spacecraft separated by a distance comparable to electron kinetic scales in the directions parallel and perpendicular to the ambient magnetic field.

3.2 Shock physics

Electron scale processes and their spatial variations, MMS provides the unique opportunity to study shocks even at electron scales. Such research has been extremely successful, but key unexplored questions remain.

3.2.1 What is the physics of the bow shock on all kinetic scales? Kinetic processes associated with the bow shock provide an environment ripe for further exploration by MMS. Only MMS offers the opportunity to observe key processes from ion scales down to electron scales. The studies proposed here provide closure to pressing science questions awaiting measurements by an MMS-like precision tool.

3.2.1.1 How do foreshock transients and subscale structures evolve, and how do they relate to particle acceleration? Foreshock transients are ion-kinetic phenomena that develop in the ion foreshock region upstream of supercritical, collisionless shocks. An assortment of foreshock transients has been identified, including hot flow anomalies (HFAs), foreshock bubbles (FBs), cavitons, cavities, and short large amplitude magnetic (SLAM) structures. Because of their large perturbations in dynamic, thermal, and magnetic pressures, foreshock transients can disturb the bow shock, magnetosheath, magnetopause, and consequently the magnetosphere-ionosphere system. The evolution of foreshock transients is still poorly understood, and without an understanding of their formation mechanisms we cannot quantitatively couple them into shock models and space weather models. FBs and HFAs, the two most significant foreshock transients, can only be distinguished by their observational characteristics. To determine their evolution, three-dimensional shape, and particle response over time, multi-point observations with separations comparable to their various spatial scales are required (Fig. 3.3). In addition, particle acceleration mechanisms by foreshock transients have not been fully determined. To investigate acceleration mechanisms, multi-point observations with appropriate separations are needed to determine the evolution of particle motion during the acceleration processes.

3.2.1.2 How are electrons heated, accelerated and thermalized at quasi-perpendicular shocks? In the standard Diffusive Shock Acceleration (DSA) scenario, electrons are accelerated stochastically by receiving energization ‘kicks’ multiple times while being scattered back and forth across the shock front. A

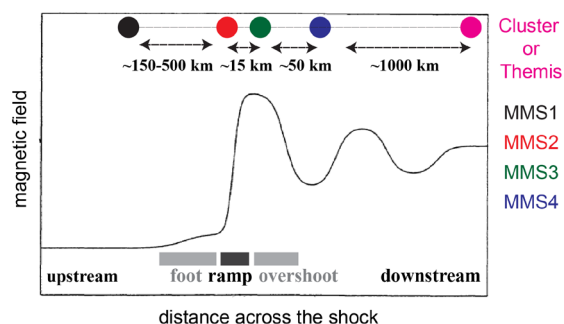


Fig. 3.3: Research on electron heating/thermalization in the Earth’s bow shock facilitated by an MMS string-of-pearls configuration. A similar configuration could be used for foreshock transients.

challenge is that electrons need to be sufficiently energetic (and non-thermal) before being injected into the standard process for further energization. While earlier in-situ observations in space suggested that Shock Drift Acceleration (SDA) is a key process of electron energization out of the thermal plasma pool, it has also been recognized that SDA needs to be combined with an additional stochastic process to explain the observed power-law energy spectra. Previous observations of intense wave activities in the shock transition region indicated that the electric and magnetic field fluctuations should provide additional electron heating/cooling and thermalization through wave-particle interaction processes. In particular, efficient scattering by electric and magnetic field fluctuations may potentially explain the observed isotropic electron heating in supercritical quasi-perpendicular shocks. MMS measurements have allowed us to determine properties and address origins of electromagnetic and electrostatic waves/structures observed in quasi-perpendicular and oblique shocks. These studies have also demonstrated that the observed waves/structures may indeed efficiently heat, pitch-angle scatter and thermalize electrons. The critical problem is to understand the relative contributions and interplay of DC-fields and wave activities in electron heating and thermalization. The problem is that the electron velocity distribution across a shock is formed non-locally, that is, the electron velocity distribution functions (VDF) measured in a particular region actually corresponds to electrons coming from other parts of the shock transition region including upstream, foot, ramp and downstream regions. Simultaneous measurements of waves and electron VDFs in different parts of the shock transition region are therefore necessary

to separate the effects of waves and DC-fields and thereby resolve the problem of the electron heating and thermalization in collisionless shocks

Researching these topics with MMS. With apogee extended to $\sim 29 R_E$, MMS provides excellent observational coverage of both the ion foreshock as well as the shock transition region. Only MMS provides the required data resolution (burst mode) and the string-of-pearls configuration (Fig. 3.3, §5) to resolve the evolution of foreshock transients and the electron physics at the shock front. Observations are directly compared to tailored numerical models; MMS determines heretofore inaccessible key quantities of the spatiotemporal nature of the development and evolution of foreshock transients and of nonlocal effects of electron energization.

Extensions via the HSO. MMS observations can be augmented by observations of the pristine solar wind from ARTEMIS and observations of the magnetosheath, magnetopause, and inner magnetosphere from THEMIS, Cluster, and other HSO assets. Such global-scale multipoint studies allow for the investigation of the impacts of foreshock transients and shock dynamics on Earth's magnetosphere-ionosphere system. During 2021-2023, THEMIS and Cluster in the dayside season provide many conjunction opportunities with MMS – for example, the THEMIS and MMS orbits are aligned in 2021-2022. When a foreshock transient is observed by multiple missions, its evolution and spatial structures are investigated on multiple scales.

3.2.2 What is the kinetic physics of interplanetary shocks and co-rotating interaction regions? Interplanetary (IP) shocks tend to be weaker than planetary bow shocks. Hence, they provide opportunities to investigate a wide range of shock parameters down to the subcritical regime where resistive-like and/or dispersive processes could account for the required energy conversion. IP shocks are also larger scale, which facilitates the creation and evolution of extended foreshock regions populated by shock-energized particles. Corotating interaction regions (CIRs), formed by the interaction of a stream of high-speed solar wind with the preceding slower solar wind, drive shock waves which expand away from the stream-stream interface. It has been suggested that the enhanced solar wind temperature, magnetic field turbulence and higher Alfvén speeds in the trailing edge of the CIR may be conducive to

particle acceleration from the tail of the solar wind distribution. Researching this broader category of shocks and discontinuities provides a unique opportunity to understand the nature of the cross-shock electrostatic potential and to address the following questions:

- *What fractions of the cross-shock potential are provided by kinetic-scale and/or nonlinear electric fields?*
- *What role do wave-particle interactions play in particle acceleration and/or energy dissipation at subcritical IP shocks?*
- *What is the spatial structure and temporal variability of IP shocks and CIRs; how does that structure influence shock acceleration and interaction with the Earth's bow shock?*

Researching these topics with MMS. The only MMS IP shock measurements (Fig. 3.4) so far largely confirmed, previously understood or theorized characteristics of supercritical shocks; however, they suggest the types of insight that could be gathered for additional IP shock events at lower, subcritical Mach numbers. In the extended mission, MMS is likely to encounter more shock events as it spends longer durations in the solar wind upstream of the bow shock. During this rising phase of the solar cycle, the interplanetary medium is dominated by persistent, clean CIRs providing at least 10-15 IP shock observations. Solar observations provide some predictive capability on a time scale of weeks to target short campaigns. MMS capabilities answer the primary questions related to kinetic processes, electromagnetic fields and waves, and shock acceleration. The likelihood of encountering these discontinuities is enhanced during designated campaigns or during campaigns conducted in coordination with Parker Solar Probe.

Extensions via the HSO. MMS measurements are the core element of investigation of the nonlocal shock and CIR structure when combined with observations from ACE, Wind, and ARTEMIS. Non-planarity and non-stationarity on these scales has an impact on particle trapping and acceleration both at the IP shock and its interaction with the bow shock.

3.3 Kinetic turbulence

The question of how plasma turbulence behaves on ion and electron scales is one of the most compelling problems in space plasma physics. The magne-

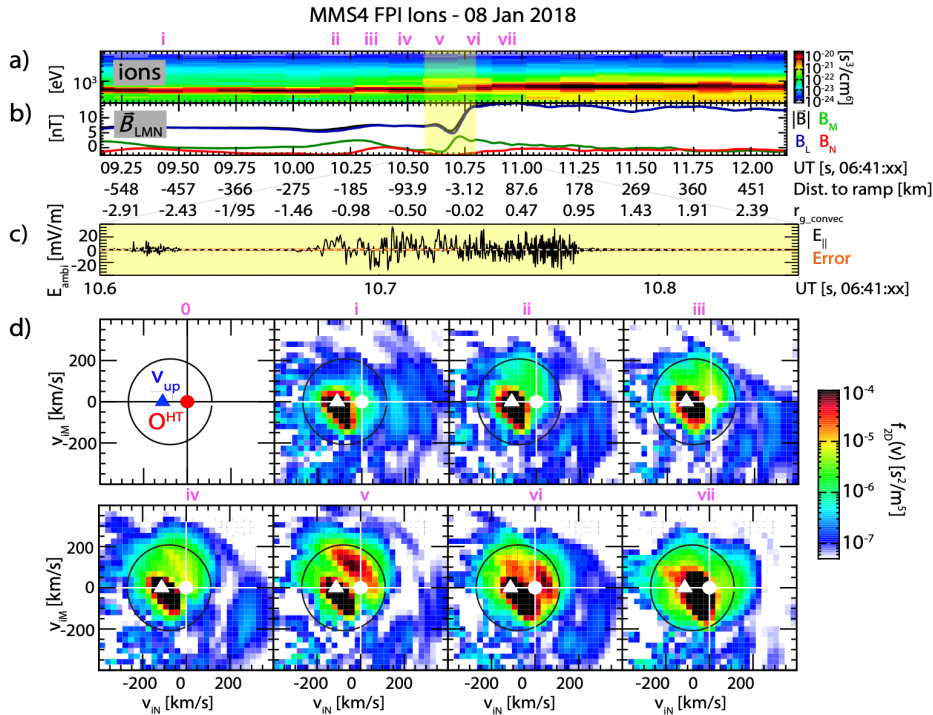


Fig. 3.4: Understanding interplanetary shocks. Using its high-temporal resolution particle capability, MMS resolves near-specularly reflected ions at an interplanetary shock (panels b and d). The novel burst-mode-resolution 3D electric field observations (panel c) also reveal very small-scale, possibly nonlinear structure within the shock ramp itself (panel a).

tosheath is an excellent laboratory for this research, and MMS offers the capability to address all relevant kinetic scales.

3.3.1 What are the drivers and evolution of magnetosheath turbulence and magnetic reconnection. Observations from Cluster and MMS demonstrate that magnetosheath turbulence tends to have a short MHD-scale inertial range compared to the solar wind. Turbulence features non-uniform properties across the magnetosheath with shallow power laws near the bow shock and more fully developed “-5/3” power laws on the flanks. It forms a multitude of thin current structures, which can be sites for magnetic reconnection. Recent MMS observations have revealed that a novel and unexpected form of reconnection in which ion jets do not form, known as “electron-only” reconnection, occurs within magnetosheath turbulence. MMS has also shown that reconnection events form in the transition region immediately downstream of the bow shock. While we know that turbulence appears to become more fully developed as plasma flows away from the shock, the role of solar wind turbulence processes at the shock, and magnetosheath transients, such as jets,

in generating the turbulence remains unclear. The early onset of reconnection at the shock may play an important role in developing the sub-ion-scale turbulent cascade, as suggested by simulations. The Taylor “frozen turbulence” hypothesis cannot be easily employed to examine scales comparable to the system size; therefore, simultaneous measurements at different distances from the shock are required to explore these processes.

3.3.2 How do large-scale turbulence properties influence magnetosheath reconnection? – Reconnection sites formed by turbulence

are fundamentally anisotropic structures, with short length scales comparable to the electron inertial length and much longer length-scales along the outflow and guide-field directions, which are controlled by large-scale turbulence properties. Simulations show that the length of the current sheets along the outflow direction determines whether ion jets form or if electron-only reconnection occurs. Estimates of the magnetic correlation length from observations using the Taylor hypothesis are consistent with this picture. However, direct measurements of 3D anisotropy of turbulence at large and small-scales are necessary to form a complete picture of how turbulence generates electron-only reconnection.

Researching these topics with MMS. A string-of-pearls configuration with varying separations, e.g., 30 – 500 – 12,000 km on the outgoing and ingoing legs of the orbit, is used to explore the evolution and driving of magnetosheath fluctuations as they propagate from the bow shock. This range of scales extends from sub-ion scales to roughly half the width of the subsolar magnetosheath, providing simultaneous measurements at multiple distances from the bow shock. Burst intervals are collected

downstream of the quasi-parallel and quasi-perpendicular shock to contrast the evolution in these two regimes. In a second possible configuration, an ion-scale tetrahedron (§5) is used to characterize the large-scale structure of reconnecting current sheets in the magnetosheath. This separation, which is larger than the ion scales and shorter than the correlation length ($\sim 10\text{-}20$ ion inertial lengths), allows the 4 s/c to sample the same current sheets and characterize the large-scale structure. Research is further enhanced by kinetic modeling. Regarding reconnection events, we know from experience that only high-resolution measurements from MMS readily permit the identification of reconnecting current sheets. MMS resolves turbulent energy propagation into the kinetic regime, and shows how turbulence interacts with transient reconnection.

Extensions via the HSO. HSO enhances the extended mission by providing larger-scale context for the MMS observations. Missions such as ARTEMIS, Wind, and DSCOVR, provide upstream solar wind conditions for bow shock and magnetosheath observations from MMS. THEMIS and CLUSTER provide magnetosheath measurements at locations off the MMS separation direction during the string-of-pearls configuration, which are helpful to examine confined transient events such as magnetosheath jets and provide large-scale context for turbulence observations in the tetrahedron configuration.

3.4 Kinetic structures shaping the magnetospheric flank

The flanks of the magnetosphere are the sites of KH instabilities, which form twisted flux tubes with only partially explored kinetic substructures. These phenomena are of great importance for solar wind-magnetosphere coupling and can only be studied by MMS measurements.

3.4.1 What are kinetic substructures of Kelvin-Helmholtz (KH) vortices? Recently, MMS (160 km spacecraft tetrahedron) demonstrated magnetic reconnection ion exhausts coming from an electron diffusion region in a Kelvin-Helmholtz vortex-compressed magnetopause current sheet (Fig. 3.5). It was also found that turbulence is present between compressed KH-associated magnetopause current sheets early in the KH evolution, sunward of the terminator. While non-linear KH growth at MHD scales is well-established along both flanks, several

aspects of the instability are not well understood. These aspects include cross-scale physics of KH-associated current sheet evolution, the onset of KH turbulence at the Earth's magnetopause, and global dawn-dusk differences. For cross-scale physics and evolution, it is not clear how much reconnection at ion scales and/or sub-ion scales (including electron only reconnection) contribute to plasma mixing in the different stages of KH evolution. For KH turbulence, MHD and kinetic simulations suggest that onset of turbulence, and ultimately KH vortex collapse, could be attributed to secondary instabilities, or alternatively that ambient fluctuations (either turbulent or particular modes) have a significant impact on the development of the KH vortices and the observed early onset of turbulence within the vortices. For global differences, it is not clear how different local flow shear on the two flanks impact KH evolution and induced current sheets.

3.4.2 What are the mechanisms of dawn-dusk asymmetries of the magnetopause current sheet? An interesting property of the terrestrial magnetopause

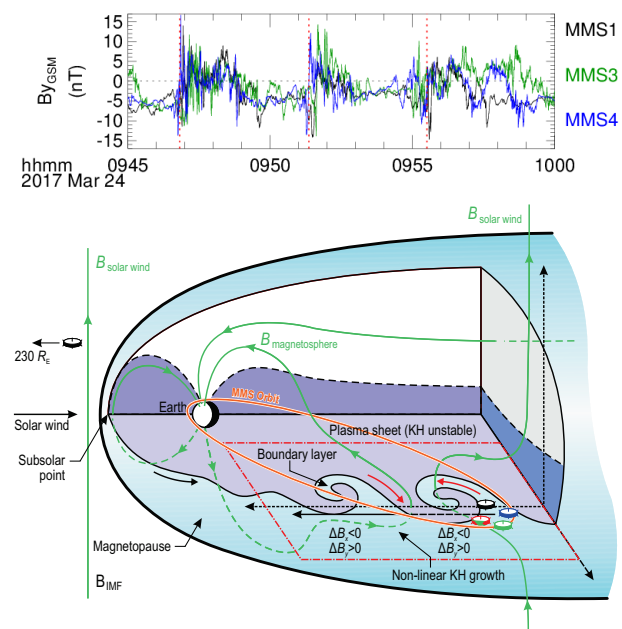


Fig. 3.5: Understanding the kinetic structure of Kelvin-Helmholtz vortices. (Top) MMS magnetic field observations of periodic, compressed current sheets (marked) at the dawnside terminator in agreement with large-scale KH waves. (Bottom) Three-dimensional cut-away view of the Earth's magnetosphere with the Sun to the left, indicating where MMS studies the kinetic structure of nonlinear KH vortices.

is the presence of a persistent dawn-dusk asymmetry in many macroscopic parameters, including current density and current sheet thickness; the dusk magnetopause is on average thinner and has a higher current density than its dawn counterpart. There are two main theories to explain the dawn-dusk asymmetry: First, external influences, like the very different nature of the bow shock at dawn and dusk result in differences in the upstream magnetosheath properties at dawn and dusk.

Researching these topics with MMS. The 29 R_E apogee is ideal for investigating all aspects of KH evolution from early onset and linear evolution sunward of the dawn-dusk terminator to the non-linear roll-up phase and proposed turbulent collapse. A string-of-pearls configuration with logarithmic 15000-650-30 km spacecraft separation (§5) provides a unique opportunity to investigate all scales (MHD, ion, electron) inherent to KH vortex onset and evolution.

Extensions via the HSO. The extended mission investigates system-scale KH and current-sheet structure science by sampling one magnetopause flank region as Geotail samples the opposite magnetopause flank. The system-scale objective determines whether both flanks typically support KH for the same upstream solar wind driving conditions despite expected shear flow differences of the local magnetopause. System-scale science of this type can also be performed during spacecraft conjunctions on the same flank. Conjunctions such as those between MMS and Geotail on 15 June and 1 July 2022 (Fig. 3.6), in which one spacecraft skims the magnetopause while another observes the upstream magnetosheath, probes the influence of magnetosheath dynamics on the development of the KH instability.

3.5 Kinetic structures in the magnetosphere

The magnetosphere is structured by larger regions, which are separated by kinetic-scale, thin, boundary layers. These layers play a key role understanding magnetospheric structure and dynamics, and their structure and evolution is poorly understood. A precision microscope like MMS is the ideal tool to research their formation and evolution.

3.5.1 What roles do wave-particle interactions have at dipolarization fronts? Magnetic reconnection and dipolarization fronts (DFs) are two of the most important phenomena commonly detected near the

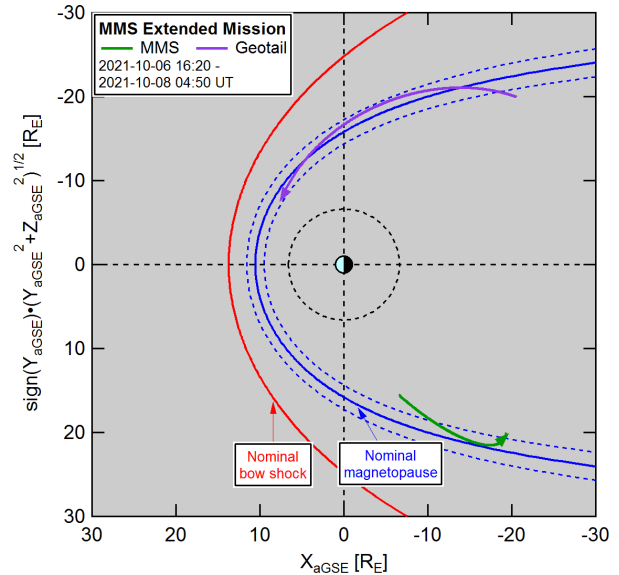


Fig. 3.6: Exploiting conjunctions with HSO assets. Example heliospheric observatory conjunction with MMS skimming the magnetopause on one flank and Geotail skimming the magnetopause on the other flank. The conjunction lasts more than 1.5 days, providing ample opportunity to observe the development and dynamics of KH instability on both flanks.

equatorial plane of the Earth's tail plasma sheet. DFs host a number of plasma waves at multiple scales associated with kinetic boundary layers arising from both processes. DFs travel macroscale distances ($> R_E$) and often display ripples caused by various instabilities with wavelengths ranging from sub-ion to MHD scales. These intrinsic multi-scale structures drive various wave modes and turbulence. Recent MMS observations showed that the nongyrotropic electrons associated with EDRs generate upper hybrid waves and electron Bernstein waves. Density and pressure gradients across DFs or reconnection separatrixes also facilitate the excitation of the lower-hybrid mode. These waves, typically propagating in the cross-tail direction, significantly regulate the energy conversion occurring in the reconnection sites, and DFs and can affect the evolution of both processes. Furthermore, MHD instabilities such as interchange and KH instabilities, which also propagate in the cross-tail direction, cause macroscopic undulations on sub-MHD/MHD scales. It remains unsolved how these multi-scale waves driven by reconnection and DFs are coupled to affect particles, energy conversion, and the evolution of the structures, i.e., how electron, ion, and fluid structures are

coupled and evolved via multiple instabilities.

Researching these topics with MMS. Finding the missing link between multi-scale structures and multi-scale waves requires a cross-scale investigation using the four MMS spacecraft with an evolved tetrahedron configuration (see §5). Two spacecraft separated by an electron scale enable us to investigate the waves modes that are most responsible for the energy conversion between the fields and particles occurring within the electron scale structures and their effects on the evolution of the electron-scale structures embedded in a DF or X-line. The other pair of MMS with a sub-ion scale separation between the two spacecraft enables us to identify sub-ion-scale structures, such as ripples generated by the lower-hybrid drift instability formed on the typically assumed planar DFs and azimuthally-invariant X-lines, as well as their effects on particle energization and temporal evolution of the structure. Finally, the two sets of paired MMS spacecraft separated by sub-MHD scales provide cross-scale investigations, enabling us to address sub-MHD scale structures in association with interchange instability, and flow vortices. By incorporating the electron, sub-ion, and sub-MHD scale measurements and by comparing to modeling results, we can address how multi-scale structures of DFs and reconnection can maintain their coherency and advance couplings among the electron, ion, and fluid scales, in a self-consistent way. This research leads to a comprehensive micro-to-macroscopic picture of wave-plasma interactions and feedbacks between these interactions and multi-scale structures.

Extensions via the HSO. The extended MMS mission with our new configuration works synergistically with the THEMIS, Cluster, and Geotail missions, all of which fly in orbits traversing the magnetotail current sheet. With MMS measurements at the core, and covering the apogee range from ~ 30 to $-9 R_E$, they enable unparalleled exploration of a full-time history of the generation, evolution, and decay of dominant waves influencing particle energization and multi-scale structures.

3.5.2 How is the plasma sheet boundary layer structured on electron and ion scales? The plasma sheet boundary layer (PSBL) is a dynamic region ripe for the growth of strong field-aligned currents, which through various instabilities can form kinetic structures such as phase-space holes and double layers

(DLs). The three-dimensional structure of electron phase space holes has successfully been measured by MMS in the PSBL (Fig. 3.7), and THEMIS and the Van Allen Probes have encountered double layers in this region, which has a net electric potential. Prior to MMS, establishing constraints on DL properties such as electric potential was limited by relatively short-baseline interferometry by single spacecraft, which excludes a potentially large portion of fast-moving structures. A direct causal relationship between double layers, plasma beams, and energy transport in the PSBL could therefore not be confirmed. The impact of double layers on large-scale magnetospheric dynamics is coupled to their total potential, rate of occurrence, lifetime, and perpendicular extent across magnetic flux tubes. Few of these properties are well constrained on either statistical or individual bases. For instance, cross-sectional area is a key property in estimates for DL influence on plasma sheet flux tubes – but it has not yet been measured directly. Occurrence rate is likely enhanced during stormtime, but more statistical data is required for confirmation. Well-resolved, 3D measurements of PSBL kinetic structures are required to understand their role in one of the most important transport regions in the magnetosphere.

3.5.3 What is the structure and evolution of the thin, pre-onset, current sheet? We have known for quite some time that the magnetotail current sheet thins down considerably prior to the onset of a sub-storm. This fact is suggestive of a causal relationship between current sheet thinning and the removal of electron magnetization by the normal magnetic field, which is needed for the onset of magnetic reconnection. Knowledge of the structure and evolution of these layers has been elusive beyond Geotail findings that the current in these layers is primarily carried by electrons. Researching their kinetic structure and evolution is all the more important as modeling has shown that electrons can become demagnetized in these layers if they are thin enough, even if no additional fluctuations are present. Fluctuations can be generated by a variety of different kinetic instabilities, or by larger scale waves or current sheet flapping. Any of these fluctuations can, in principle, also demagnetize electrons or contribute to demagnetization. In order to understand why and when reconnection occurs in the magnetotail, we need to observe these current sheets during all

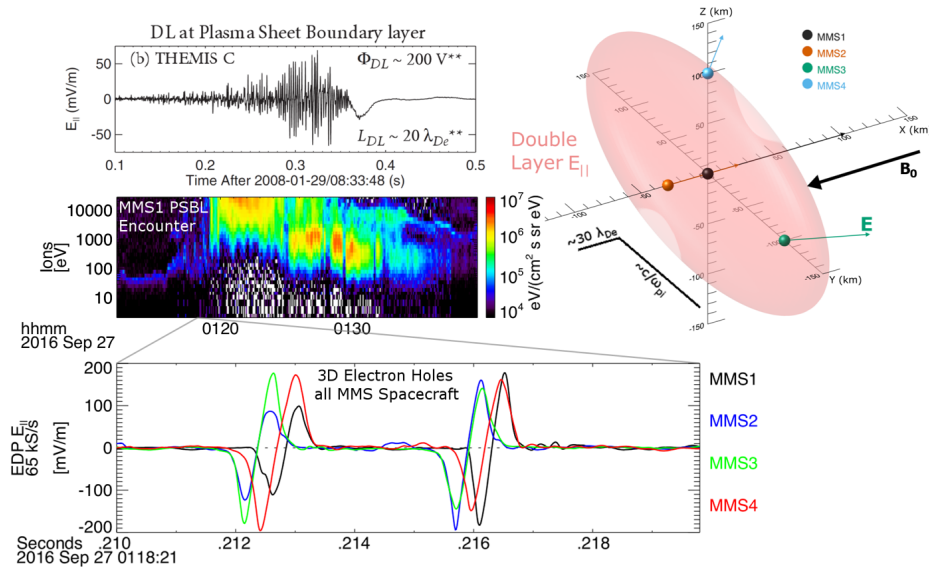


Fig. 3.7: Understanding the kinetic structure of the PSBL. (Top) Pre-MMS double layer observation at the PSBL. (Right) MMS formation (colored spheres) designed to resolve all relevant scales. Vectors represent possible electric field measurements. An idealized double layer E_{\parallel} contour is rendered in red. MMS resolves 3D structures: (Center) Ion energy spectrogram from an MMS encounter with the PSBL on 2016-09-27. (Bottom) Sample of E_{\parallel} signatures from multiple electron phase-space holes observed by all MMS spacecraft at the PSBL.

limit on cross-section can be obtained. A traditional, nearly tetrahedron arrangement also retains the ability to determine velocity across thin layers such as reconnection separatrices or newly forming thin current sheets. The combination of these techniques leads to a comprehensive picture of the kinetic structure of the PSBL and pre-onset current sheets.

Extensions via the HSO. Additional association of kinetic structures with solar wind and magnetotail activity provides context for the relationship between electron-scale behavior and the

stages, from their formative phase to just prior to the onset of reconnection. In this context it is also important to identify any plasma waves that may contribute to electron demagnetization and to assess the role of pure thinning vs. wave-driven demagnetization.

Researching these topics with MMS. On magnetospheric scales, the orbit of MMS is ideally situated for long duration plasma sheet encounters within the magnetosphere, providing many chances to observe double layers and phase-space holes under various magnetospheric conditions as well as current sheet flapping, the latter particularly in a string-of-pearls configuration. An expanded tetrahedron formation (§5) with two spacecraft closely spaced along the magnetic field allows reliable estimation of the parallel velocity and electric potential. The remaining two satellites can be employed to probe larger scales in the current sheet plane, including plasma sheet thinning. Perpendicular spacing between 100 and 500 km (ion inertial scales) can probe the 3D structure of double layers and permit a direct comparison to concurrent modeling. In the case of observation by the closely spaced pair and non-detection by the perpendicular satellites, a useful upper

global picture of magnetospheric dynamics. Previous conjunctions have been successful in showing intense, electron-scale beams resulting from reconnection in the magnetotail. Many future opportunities exist for concurrent measurements by MMS, Geotail and THEMIS in the PSBL to study current sheet thinning on a combination of kinetic and macroscales in the magnetotail as well as providing context by looking for signs of reconnection, bursty bulk flows, and DFs.

3.6 Particle acceleration

Understanding particle acceleration remains a compelling objective owing to relevance to space weather and its general importance in a variety of space and astrophysical contexts. Therefore, it remains an objective of this proposal to understand particle acceleration directly or indirectly related to magnetic reconnection, and to contribute to understanding acceleration of radiation belt particles and of energetic particles of solar origin.

3.6.1 What are the scale sizes and driving conditions of electromagnetic ion cyclotron (EMIC) and ultra-low frequency (ULF) wave activity? Wave-particle interactions are critical to particle dynamics

in Earth's inner magnetosphere. EMIC waves are driven by temperature anisotropy of energetic ions and acquire their dispersive properties based on ion composition. EMIC waves are considered critical for the loss of radiation belt electrons with energies in the several MeV range. ULF waves, such as standing Alfvén waves and cavity/waveguide modes, are regularly observed in the inner magnetosphere and can be driven externally by pressure fluctuations in the solar wind and along the magnetopause or internally by mechanisms such as drift-bounce resonance with trapped particles. These ULF waves are important for, among others, radiation belt transport and acceleration. The active regions of EMIC waves have only been characterized statistically, and there is still very little understanding of how large the EMIC active region is for any particular period of activity. The best data so far has been with 2-point Van Allen Probes (VAP). Past ULF wave observations have had difficulty quantifying the mode number and other key properties of ULF waves owing to a lack of appropriate satellite conjunctions – information critical to assessing their transport and acceleration role. The provision of this knowledge requires multipoint observations.

3.6.2 What are the plasma sheet sources of Earth's radiation belt electrons? The dominant source of relativistic (i.e., $> \sim 500$ keV) electrons in the outer radiation belt is localized acceleration of a seed population of 10s to 100s of keV electrons by whistler mode chorus waves. The source of chorus waves is anisotropic distributions of keV to 10s of keV electrons, primarily injected from a source in the plasma sheet during substorm activity. Despite the array of discoveries and new understanding from VAP, there are still outstanding questions about the connection and energy dependencies between substorm injections, chorus waves, and the sources of outer radiation belt electrons, and whether all substorm injections result in an enhancement in whistler-mode chorus activity in the inner magnetosphere. Answering these questions requires simultaneous, multipoint observations including spacecraft in both the outer radiation belt and the near-Earth plasma sheet.

Researching these topics with MMS. MMS provides 4-point observations with unprecedented temporal resolution and instrumentation to study the nature of EMIC and ULF waves in Earth's inner magnetosphere. Electron phase-space density distri-

butions derived from FEEPS and EIS are used to study wave scattering by EMIC waves. MMS data can further be used for multipoint studies of the connection between source populations of electrons in the near-Earth plasma sheet, substorm injections, chorus wave activity in the inner magnetosphere, and outer radiation belt enhancements. MMS is the only mission that can provide particle distributions over a critical range of energies (i.e., in the 10s to 100s of keV range) simultaneously from within the heart of the outer belt into the near-Earth plasma sheet. It will therefore provide entirely new understanding of the evolution of source populations.

Extensions via the HSO. MMS plus Arase (ERG) and/or Cluster conjunctions can be used to examine the propagation characteristics and modulation of EMIC waves from their generation region near the magnetic equator (MMS) to higher latitudes (Arase and/or Cluster); the effects of the cold and hot ion composition on EMIC wave propagation as informed by these missions will be key to such a campaign. MMS combined with Arase, Cluster, Geotail, and THEMIS can be used to examine the active regions of EMIC and ULF waves. Furthermore, MMS-based research can be supported by Arase to study these radiation belt questions plus additional ones on loss of radiation belt electrons. When MMS is combined with assets observing radiation belt losses at LEO, studies of EMIC waves resulting in radiation belt electron losses can be examined and theories tested with unprecedented detail.

3.6.3 How does energetic ion acceleration in the magnetotail depend on ion species? A combination of particle simulations with Cluster, THEMIS, and MMS observations has advanced our understanding of ion, specifically proton, acceleration in relation to reconnection, flow bursts, and the collapse of the inner tail (dipolarization). Acceleration near an X-line is relevant for ion beams near the plasma sheet boundary (as discussed below). One might distinguish three regions with characteristically different ion properties: PSBL, central plasma sheet (CPS), and precursors ahead of earthward propagating DFs.

- PSBL: Reconnection at an X-line, as well as at a propagating DF may be the cause of ion beams near the plasma sheet boundary. The combination of such a beam with a reflected beam is useful for estimating the distance to the reconnection site. This technique breaks down farther inward

(or later in an event) when the Earthward and reflected tailward beams are no longer accelerated at the same site. Multiple Earthward and tailward beams may result from multiple encounters with a propagating DF as well as from the X-line and mirroring near Earth.

- CPS: Proton distributions behind a DF are characterized by perpendicular anisotropy, probably from betatron-like acceleration at and within a DF. Low-energy field-aligned beams are likely to be present within the main population. Their presence needs to be established and investigated.
- Precursor ions: Ions at tens of keV preceding a DF may result from reflection of lower energy ions originating from the pre-existing CPS.

As indicated by particle tracing, the relatively cold field-aligned beams in the CPS presumably come from the PSBL or the lobes and are accelerated by first-order Fermi acceleration (current sheet acceleration), which needs confirmation by better counting statistics on short time scales.

Researching these topics with MMS. As pointed out above, the cross-tail extent of the acceleration region is comparable to the gyroradius of energetic ions. Similarly, the thickness of the current sheet within which the ions are accelerated can be comparable to the ion inertial length or gyroradius. Increasing the MMS tetrahedron scale to ion scales will thus provide new insights into the properties and mechanisms of the ion acceleration.

Extensions via the HSO. Additional assessments of ion acceleration are possible by the larger-scale context provided by the HSO. Previous conjunctions have already been successful in researching electron beams. Many future opportunities exist for concurrent measurements by MMS, Geotail and THEMIS in the PSBL for studying ion acceleration processes in different regions and contexts.

3.6.4 In which way is the physics of the Cusps and Associated Diamagnetic Cavities (DMCs) related to energetic particle acceleration? Magnetosheath plasma has the most direct access to the ionosphere through the high-altitude cusps owing to magnetic reconnection operating in the vicinity of the exterior cusp funnel. Cusp signatures differ depending on altitude and IMF orientation. The four spacecraft Cluster mission revealed the general structure of the high-altitude cusps on ion scales. Recently (Fig. 3.8) MMS detected the presence of energized and trapped O^+

from the ionosphere and trapped He^{++} from the solar wind at the high-latitude magnetopause. These observations were used to determine the distance from the MMS spacecraft to the reconnection site and to assess the size of the inferred magnetic bottle. To address the nature (e.g., reconnection rate) and global consequences of magnetopause reconnection, MMS observations through the cusp funnel and analysis of ion dispersions with composition measurements are needed. String-of-pearls MMS observations of the cusp help distinguish the relative contribution of the suggested sources for the high energy particles observed in the cusp-associated DMCs: 1) local acceleration via 'turbulence' in DMCs, 2) quasi-parallel bow-shock, 3) magnetospheric source, or 4) local acceleration via particle trapping and drifting in a reconnection quasi potential.

Researching these topics with MMS. From 2021 to 2025, the apogee latitude increases, and cusp and high latitude magnetopause encounters increase (see also §5). The full complement of high-resolution fields and particle measurements combined with energetic particle and composition measurements enables cusp physics and formation of the cusp associated DMCs to be understood from ion to electron scales. The string-of-pearls configuration is ideal for tracking the motion of the reconnected field lines through the cusp, establishing the formation of the DMCs, and distinguishing between different proposed acceleration mechanisms and particle sources.

Extensions via the HSO. Having four MMS spacecraft in the high-altitude cusp region in the string-of-pearls configuration while having THEMIS at the low-latitude dayside magnetosheath-magnetopause, and Geotail or ARTEMIS upstream of the bow shock provides additional opportunities to directly relate solar wind, bow shock, magnetospheric, and locally accelerated sources of plasma in the cusp.

3.6.5 What is the Long-Term Behavior of Pickup Ion Composition and Dynamics at 1 AU? The existence of two major populations of pickup ions (PUIs), interstellar and inner source, is well-documented. In-situ measurements of helium at 1 AU and hydrogen at 3 AU agreed well with predictions. While the existence of these ion populations is firmly established, there is yet much to be understood about them. For interstellar pickup ions, the following questions are important: 1) Are there focusing cones that exist for minor ion species like oxygen and neon (Fig. 3.9)?

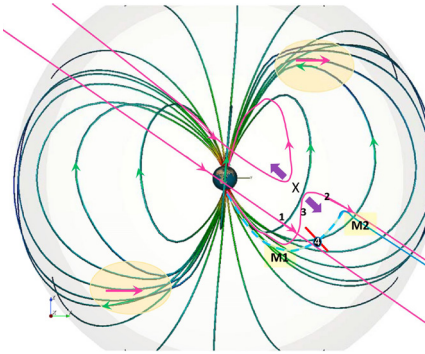
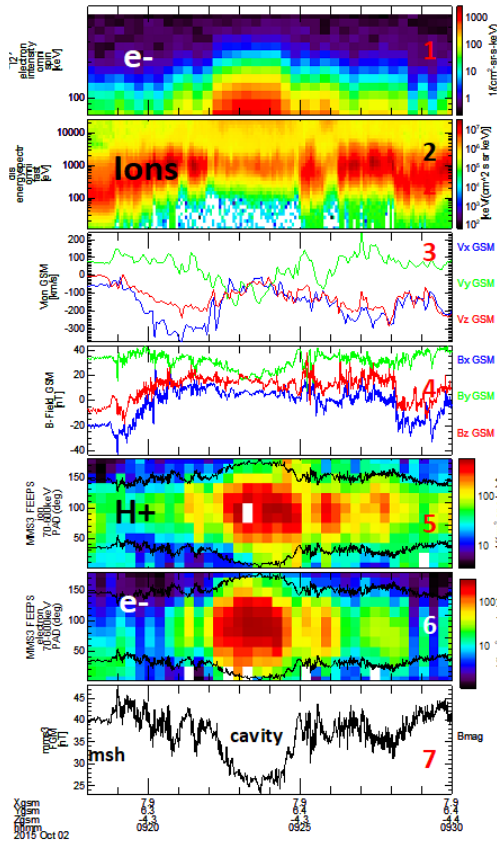


Fig. 3.8: MMS researches particle populations in the cusp. (Left) MMS1 observations of the plasma and magnetic field properties. The loss cone pitch angle is highlighted by black lines for energetic protons (l) and electrons (m), showing the presence of a trapped population of energetic particles in a magnetic bottle. (Top) MMS trajectory through the high-latitude DMC-like cavity formed by low-latitude reconnection. Figure is adapted from Nykyri et al. (2019).

2) How does the solar cycle affect the formation/distribution of these ions? 3) How do turbulence conditions, generated in the solar wind or by the interaction with the Earth’s foreshock, affect the kinetic properties of these ions? For inner source pickup ions important questions include: 1) What is the temporal variability of the inner source PUIs (Fig. 3.9)? 2) How are these ions affected by variations in the Solar Radiation Environment? These sets of questions have far-reaching implications, particularly with how these interactions can assist with understanding how the solar environment interacts with the near interstellar (NISM) medium.

Researching these topics with MMS. The 29 R_E apogee of MMS allows extensive temporal and spatial surveys of the SW environment and SW-bow shock interaction region. The large geometric factors of the plasma instruments ensure that MMS can provide the required full coverage surveys of species-resolved ion velocity distributions more rapidly than any other instrument currently deployed. Turbulence effects on the PUIs are investigated with the high time resolution of the magnetometers, providing a completely new look at pickup ions at 1AU.

connection, shocks, waves, and turbulence in the space plasma environment at Earth, MMS science is at the heart of NASA’s Heliophysics goals.

The MMS mission has yielded outstanding advances towards all of the goals, G1-G3, especially within the main scientific target for the mission, magnetic reconnection. Great strides have been made not only in uncovering the inner workings of magnetic reconnection itself. How reconnection works to directly link different heliophysics domains and the surprising roles it plays in other energization and transport processes, such as shocks and turbulence, have also been revealed. As the dominant process behind both the eruptive events and large-scale energy conversion processes that drive space weather, the enhanced understanding of magnetic reconnection facilitated by MMS is critically important for improving our knowledge of and capability to predict extreme space environment conditions.

In the extended mission MMS pursues high-level science goals designed to continue and expand the crucial contributions of the mission to all of the overarching heliophysics goals. Most directly, key advances on G1 will result from studies of mag-

Extensions via the HSO. IMAP, due for launch in 2024, is the next mission slated for this research. A continuous record of PUIs at 1 AU from solar minimum (MMS) through solar maximum (MMS and IMAP) provides a unique opportunity to answer solar cycle-dependent questions on the dynamics of interstellar atoms in the heliosphere.

4 Relation to NASA’s Strategic Plan

4.1 Relevance to NASA’s Heliophysics Strategic Goals

Targeting the fundamental physical processes of magnetic re-

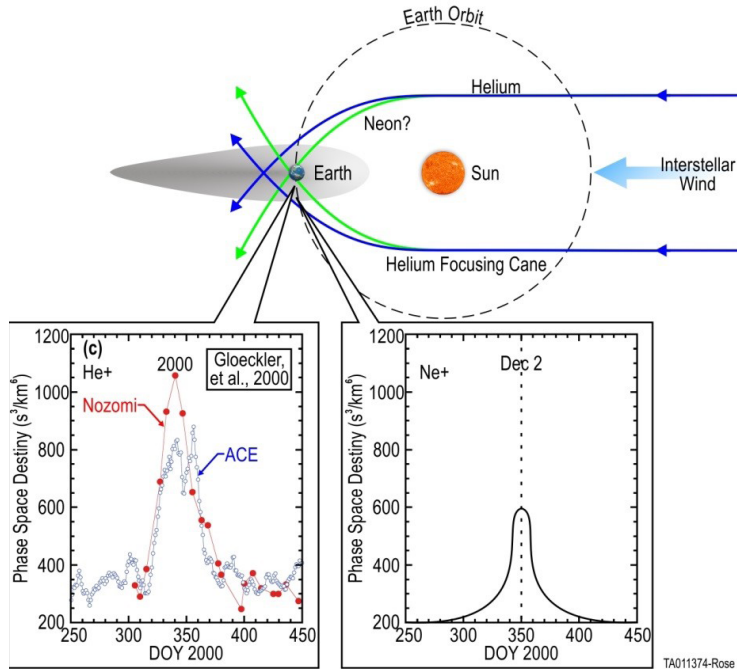


Fig. 3.9: Investigating the Focusing Cone at 1 AU by MMS. Investigations of Solar Cycle effects on the PUI populations are possible in the extended mission. Interstellar and Inner Source ion populations observed during these periods are distinguished via their respective pitch angle distributions which require high time resolution measurements of the magnetic field.

netic reconnection, shocks, turbulence, particle acceleration, and other kinetic processes for a broader range of plasma conditions and configurations and including both electron and ion scales. The impact of cold and heavy ion populations as well the effects of transients, waves, and turbulence on the reconnection process and its efficiency as an energy conversion and transport process are major studies for the extended mission, the results of which will yield important contributions to G2. Significant contributions to G2 also come from the planned studies that concern the relative importance of reconnection, shocks, turbulence and other processes in establishing energization and transport linkages between different heliophysics domains. In fulfilment of G3, further quantification of magnetic reconnection as it operates in a broader range of conditions constitutes a critical step towards improved space weather prediction capabilities.

4.2 Role in the Heliophysics System Observatory

Throughout the extended mission, fortuitous constellations are abundant with other missions of the HSO, and beyond. Such conjunctions constitute the

basis for combined studies that significantly enhance the science opportunities for MMS as well as for the other missions involved. Specific opportunities to utilize other missions in the HSO to enhance the science return for MMS have been emphasized in the descriptions for each of the science objectives. Some examples of particularly promising constellations are discussed and illustrated in §5.

Joint campaigns with the Parker Solar Probe mission arranged around promising conjunctions constitute a prominent example of future opportunities. Through such campaigns, MMS provides a uniquely capable near-Earth complement to investigations of the formation, propagation, and development of interplanetary shocks and other heliospheric structures as well as solar energetic particles and their entry into the magnetosphere. The high-resolution capabilities and comprehensive measurement suite of MMS add a highly valuable kinetic physics component to these studies. MMS plays a similar important role

for other solar and heliospheric missions, including notably the upcoming Solar Orbiter mission. For investigations of the solar wind magnetosphere interaction and large-scale magnetospheric dynamics carried out by the constellation of THEMIS/ARTEMIS, Cluster, Geotail, and other missions, MMS provides a crucial additional node possessing a distinct multi-point, kinetic scale-resolving capability.

Opportunities for joint observations and campaigns to utilize conjunctions in support of science investigations being led by other missions in the HSO are actively sought by the MMS Team.

NASA's Heliophysics goals, as described in the 2014 SMD strategic plan, are:

- G1: Explore the physical processes in the space environment from the Sun to the Earth and throughout the solar system
- G2: Advance our understanding of the connections that link the Sun, the Earth, planetary space environments, and the outer reaches of the solar system
- G3: Develop the knowledge and capability to detect and predict extreme conditions in space to protect life and society and to safeguard human and robotic explorers beyond Earth.

5 Implementation

5.1 Orbit and Campaigns

The MMS spacecraft are currently in a $1.8 \times 29 R_E$ orbit that precesses over 24 hours local time in approximately 1 year. Figure 5.1 shows the MMS orbits (in green) projected into the X-Y_{GSE} plane starting at the beginning of phase 6 (i.e., the start of the 6th dayside sweep of the apogee of the spacecraft, starting 9 Oct 2020). Also shown on the orbits are the predicted encounters with the magnetopause (blue) and bow shock (red) as the spacecraft apogee sweeps across the day side from dusk to dawn. In the magnetotail, parts of individual orbits are color-coded when the spacecraft are within $0.5 R_E$ of the plasma sheet (grey) and the neutral sheet (black). These times are important for magnetotail reconnection and bursty bulk flow science. The clockwise rotation of the apogee starting on the duskside provides a natural division of each year's orbits into four campaigns described in Table 5.1. Each campaign has a different science focus based on the spacecraft location, and magnetic reconnection figures prominently in all campaigns.

Not shown in Fig. 5.1 is the inclination of the orbit. Orbit perturbations over the next 5 years will torque the apogee out of the ecliptic plane, reaching a maximum inclination in 2023 and then return it to the ecliptic plane by the end of the 5 years. MMS science over the next 5 years has been adjusted to take advantage of these changes. In particular, the high inclination of the orbit combined with the time of year of the dayside sweep results in encounters with the southern magnetospheric cusp. The magnetospheric cusps were the target of the Cluster prime mission, and their investigation of ion-scale physics was one of the significant accomplishments of the mission. However, in 2023, MMS provides the first-ever observations of high-latitude magnetopause reconnection and cusp dynamics on electron-scales.

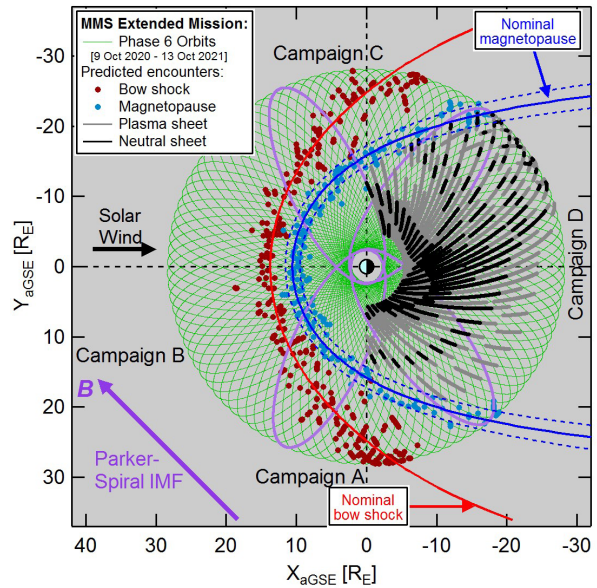


Fig. 5.1: MMS orbits for Oct 2020-Oct 2021 divide into 4 campaigns with specific science focus based on the spacecraft location. Magnetic reconnection is a focus in all campaigns.

Based on the insights provided by MMS studies of electron-scale physics at the low-latitude magnetopause, the observations at high-latitudes will prove to be equally intriguing and scientifically significant.

5.2 Configuration

The MMS spacecraft configuration is designed to maximize the science return. Different configurations are applicable to different science objectives. In the first 3 years of this senior review period, the spacecraft explore the magnetopause at increasingly higher latitudes. This exploration culminates in 2023 with encounters of the southern magnetospheric cusp. The first science goal of MMS is to: Understand how reconnection works in all boundary regions in geospace. Reconnection at high latitudes up to the southern cusp provides an opportunity to investigate reconnection in a new plasma regime.

Table 5.1: Each year of MMS orbits is divided into five campaigns that maximize mission science return.

Campaign	Approx. Duration (months)	Orbit Description	Science Topics
A	1.5	Duskside magnetopause skimming	Flank magnetopause reconnection , Kelvin-Helmholtz
B	6	Duskside magnetopause, bow shock and pristine solar wind Dawnside magnetopause, bow shock and ion/electron foreshock	Duskside/dawnside magnetosphere, dayside magnetopause reconnection , quasi-perpendicular, quasi-parallel bow shock, solar wind turbulence magnetosheath flow bursts
C	1.5	Dawnside magnetopause skimming	Flank magnetopause reconnection , Kelvin-Helmholtz
D	3	Magnetotail	Magnetotail reconnection , Bursty bulk flows, Dipolarization fronts

Thus, to connect with the multitude of results from low latitudes, the MMS spacecraft will remain in a configuration that is essentially tetrahedron for the first 3 years. This configuration is optimal for the study of magnetic reconnection. The tetrahedron configuration is optimized for the magnetopause crossings that occur approximately half-way to apogee on the outbound and inbound orbit legs.

After 2023, there are changes to the spacecraft configuration. To minimize science disruption, these changes occur over days to weeks with minimal orbit maneuvers. Table 5.2 shows the two types of configurations that enhance cross-scale Science. The log string of pearls configuration was tested during a 1-month period in February 2019 when the apogee of the constellation was raised from 25 to 29 R_E . It provides a variety of scales ranging from two spacecraft spaced at electron scales to 5 pairs of spacecraft with spacings from ion to MHD scales.

5.3 Coordination with other missions in the HSO

The four MMS spacecraft play an integral role in the Heliospheric System Observatory (HSO). All of the Science objectives in §3 are enhanced in specific ways when the MMS observations are combined with those from other elements of the HSO. The next 5 years provide some exciting new opportunities for conjunctions with the HSO where MMS science is enhanced, and MMS has the opportunity to enhance the science of other HSO elements. In particular, MMS provides unique electron-scale measurements that, when combined with other HSO elements, results in cross-scale opportunities that span micro-scales through the meso- and to the macro-scales. Figure 5.2 shows some examples of these opportunities for magnetospheric physics studies.

Figure 5.2 shows a very interesting HSO configuration with MMS in the magnetotail, which is repeated many times in the next 5 years. The armada of spacecraft are distributed over a wide range of distances down the magnetotail. MMS provides

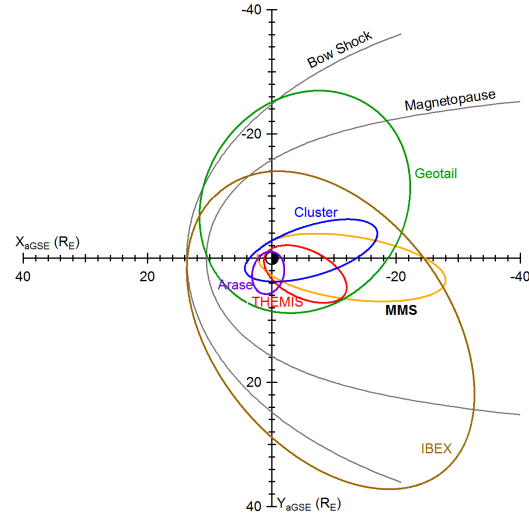


Fig. 5.2: MMS is an integral part of the heliophysics observatory, providing unique electron-scale observations. This example of many MMS conjunctions with HSO elements emphasizes the microscope-telescope science of, e.g., magnetotail dynamics during reconnection.

unique electron-scale observations of reconnection and depolarization fronts, IBEX provides neutral atom imaging of the magnetotail, and the other HSO elements study meso- and macro-scale physics of reconnection and plasmoid formation, bursty bulk flows and flow breaking in the inner magnetosphere, and dipolarization front convection and evolution.

Not shown in Fig. 5.2 are the many opportunities for coordination with elements of the HSO that are studying the Sun and inner heliosphere. These opportunities include multi-point solar wind studies combining Parker Solar Probe, MMS, and the spacecraft at L1. In addition, Sun-solar wind studies are facilitated using SDO and/or Solar Orbiter observing the Sun and MMS in the solar wind.

5.4 Instrument modes

During each ~3-day MMS orbit, science data collection occurs in Fast Survey during defined Science Regions of Interest (SROI), whereas the other portions of the orbit

are for lower resolution data gathering, calibration, and maintenance activities for the particle instruments. Burst mode

Table 5.2: After 2023, new spacecraft configurations enhance cross-scale science.		
Configuration	Description	Enabled Science Topics
Multi-scale, irregular tetrahedrons	4 or 3 spacecraft in a plane, 2 at electron scales and 2 at ion scales	3.1.2: Connecting reconnection kinetic and fluid scales 3.3.3: Instabilities and energy conversion in the tail
Logarithmic string of pearls	4 spacecraft in the orbit plane with spacing that progresses logarithmically from electron to beyond ion scales	3.2.1: Physics of the bow shock on all kinetic scales 3.3.2: Large scale turbulence influence on reconnection 3.4.1: Kinetic structure of KH vortices 3.4.2: Mechanisms of dawn-dusk asymmetries

data are also obtained in the SROIs and stored on-board. The onboard software prioritizes the burst mode data to bring to ground, and the Scientist In The Loop (SITL) has the ability to change and increase the selections, assisted by the new AI tools that have been developed to streamline this process. The planning process and rules-based scheduling system for these activities have been optimized over the course of the mission and are operating with high efficiency.

6 Technical Section: Mission Status

6.1 Instrument performance

Because very few components have been compromised and not every element is simultaneously required on each spacecraft, the nearly 100 instrumentation components continue to provide nearly full Level-1 performance (Table 6.1) and appear capable of continuing this performance. There are no open subsystem or hardware risks, providing confidence in continued reliability for a 2nd extended mission. Minor issues are detailed below.

6.2 Instrument status

All instruments are operating nominally with remarkably few exceptions (Table 6.2). Details for each instrument are:

FPI DIS/DES: The 32 Dual 16-channel ion and electron spectrometers measure 2 eV-30 keV ions and 6 eV-30 keV electrons, respectively, and deliver >95% lossless data through their compression chips. The statistical and systematic uncertainties of FPI data have been quantified, and Level-2 FPI data products regularly provide high-fidelity estimates of current densities using data from only a single spacecraft, enabling unprecedented studies of kinetic-scale physics. FPI introduced a refined energy

sweep table for solar wind observations (ions: 197 eV-9222 eV; electrons: 4 eV-940 eV).

During the summer of 2018, two of the four MMS4 dual electron spectrometers suffered HV801 optocoupler failures; both are no longer operational. One MMS3 dual ion spectrometer operates to max energy of 11 keV, with no appreciable loss to moment accuracies. Weekly monitoring indicates no further optocoupler issues. MMS maintains a near constant temperature for these detectors, which appears successful in maintaining their health even through deep eclipse. FPI anticipates uninterrupted operations throughout this extended mission.

FIELDS E-Field: Full 3D electric field measurements continue within specifications for all spacecraft. In June 2016, a micrometeoroid severed a single bias wire of Probe 4 (SDP4) on MMS4 and is no longer accurate in the frequency range DC- ~600 Hz. For this range, the FIELDS team successfully implemented a post-processing routine using the remaining probes to determine the E-field components in the spin plane. Using comparison data from before June 2016, Fig. 6.1 shows that the resulting accuracy change, remains less than the 0.5 mV/m mission success requirement with only a modest increase in the noise floor. A second micrometeoroid impact occurred in Sept 2018 to Probe2 (SDP2) on MMS2 which severed its 12V power. A flight software mod in early Oct 2018 reconfigured signals from the three remaining SDP probes to continue MMS2 spacecraft potential calculations, several burst trigger quantities, and the 1% duty cycled AC E-field, keeping MMS2 within specifications.

FIELDS B-Field: All magnetometers on all spacecraft are operating nominally.

FIELDS EDI: Some HV optocouplers in the Electron Drift Instrument (EDI) deflection system were

known before launch to exhibit a higher than desirable degradation with time. When a HV amplifier reaches the limit of its drive capability due to a degrading opto-coupler, the impact on instrument operations and science return depends on the affected system. The energy for the Ambient Electron

Table 6.1: Instrument Level 1 Performance

L1 Req	Measurement	Cadence	Range	Resolution	Angular	Met?
M10, M30	FIELDS B field	10 ms	DC – 6 khz	0.1 nT	Full 3D	✓
M20, M30	FIELDS E field	1 ms	DC – 100 kHz	0.5 mV/m	Full 3D	✓
M40	FPI Electrons	30 ms	6 eV- 30 keV	20%	12°	✓
M50	FPI Ions	150 ms	2 eV – 30 keV	20%	12°	✓
M60	HPCA Ion composition	10 sec	10 eV – 30 keV	20%	12°	✓
M70	EPD Energetic electrons & ions	10 sec	To 500 keV	N/A	12°	✓
M80	Energetic ion composition	30 sec	To 500 keV	N/A	12°	✓
I70	Potential Control	20 sec	< 4 V	< 0.1 V	N/A	✓

Table 6.2: Instrument Status																	
MMS1								MMS2									
Central Processor				DFG	AFG		SCM		Central Processor				DFG	AFG		SCM	
SDP1	SDP2	SDP3	SDP4	ADP1	ADP2	EDI1	EDI2	SDP1	SDP2	SDP3	SDP4	ADP1	ADP2	EDI1	EDI2	BField	
DIS0	DIS1	DIS2	DIS3	DES0	DES1	DES2	DES3	DIS0	DIS1	DIS2	DIS3	DES0	DES1	DES2	DES3	EField	
FEEPS1				FEEPS2				FEEPS1				FEEPS2				Electron	
EIS				HPCA				EIS				HPCA				Ions/Co	
A1E1	A1E2	A1E3	A1E4	A2E1	A2E2	A2E3	A2E4	A1E1	A1E2	A1E3	A1E4	A2E1	A2E2	A2E3	A2E4	ASPOC	

MMS3								MMS4									
Central Processor				DFG	AFG		SCM		Central Processor				DFG	AFG		SCM	
SDP1	SDP2	SDP3	SDP4	ADP1	ADP2	EDI1	EDI2	SDP1	SDP2	SDP3	SDP4	ADP1	ADP2	EDI1	EDI2		
DIS0	DIS1	DIS2	DIS3	DES0	DES1	DES2	DES3	DIS0	DIS1	DIS2	DIS3	DES0	DES1	DES2	DES3		
FEEPS1				FEEPS2				FEEPS1				FEEPS2					
EIS				HPCA				EIS				HPCA					
A1E1	A1E2	A1E3	A1E4	A2E1	A2E2	A2E3	A2E4	A1E1	A1E2	A1E3	A1E4	A2E1	A2E2	A2E3	A2E4		

Mode (AEM) was reduced from 500 eV to 250 eV in October 2019 to reduce drive currents and lower the optocoupler degradation rate. The estimated remaining run-time hours for each is carefully time managed. Table 6.3 summarizes the current status.

The primary functions of EDI continue unabated and essentially at full success level. The calibrations for E and B are well understood, and updates are stable over time; periodic calibrations can be expected to continue throughout the mission’s lifetime.

HPCA: At the start of Phase 1b, the RF energy range (used to reduce the high proton fluxes without affecting the heavier ion fluxes) was expanded from

the original 0.5 to ~4 keV to 0.2 to ~4 keV to reduce the high fluxes of magnetosheath protons in the energy range from 0.2 to 0.5 keV. The RF proton flux reduction for MMS1 and 2 is approximately 50% over the energy range, and the reduction for MMS 3 and 4 is approximately 90%. The spacecraft are operated differently to bracket the range of proton fluxes in the magnetosphere, boundary layers, and magnetosheath. In the magnetotail, the RF is turned off because the proton fluxes are low enough that flux reduction is not necessary. Gain tests conducted approximately every 6 months indicate that the detector microchannel plates (MCPs) have not aged and it has not been necessary to increase the MCP voltage to increase the gain in the past two years.

EPD: On January 31, 2016, one of the Energetic Ion Spectrometer (EIS) units (EIS1) turned off high voltage after sensing a micro-discharge in its high voltage circuitry. On January 31, 2018, the EIS1 high voltage was restored, and no further issues have been encountered. There

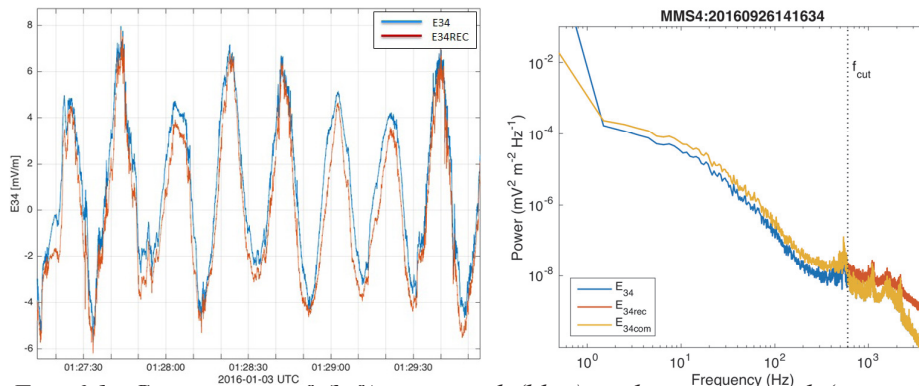


Fig. 6.1: Comparison of (left) measured (blue) and reconstructed (orange) wave forms using data taken prior to the anomaly and (right) post-anomaly noise levels of the measured (blue), reconstructed (orange), and combined (yellow) products along the SDP3-4 axis.

Table 6.3: Electron Drift Instrument (EDI) HV Optocoupler Status and Impacts

	Affected Units ¹		EDI Subsystem	EDI measurement impact	MMS Science Impact
	EDI1	EDI2			
MMS1	2	2	EDI Gun Deflection	When B is rapidly varying, loss of beam return at some spin phase	Minimal impact to frequency of E and B intra-instrument calibrations
MMS2	2	2			
MMS3	2	Sep2019			
MMS4	2	2			
MMS1	4	4	Electron beam generation	Electric field mode limited to one unit; Ambient Electron Mode continues	Currently benign
MMS2	4	Nov2016			
MMS3	May2017	4			
MMS4	4	4			
MMS1	25	25	Electrostatic optics	Potential loss of geometric factor and ability to detect signal return for poleward look directions	Fully functional
MMS2	2	25			
MMS3	4	4			
MMS4	2	2			

¹status or estimated remaining life in years at 10 hours E-Field Mode per orbit and 50% ambient electron mode

has been some light contamination in some of the Fly’s Eye Energetic Particle Spectrometer (FEEPS) detectors owing to penetration of the aluminum entrance foils that are used to prevent protons from striking the electron detectors. While the rapid burst data can easily be filtered on the ground, the project has uploaded masking tables to provide more comprehensive survey data from all spacecraft; thus, the impact is manageable. In December 2019, the energy range on one of the EIS sensors (EIS4) was shifted to much higher energies to complement the FEEPS electron data and enable additional inner magnetospheric studies after decommissioning of the VAP mission.

ASPOC: The Active Spacecraft Potential Control (ASPOC) emitters have consumed far less indium to date than expected (~15%) owing to the lower level of ion currents (10 μ A per unit), which enable high values of beam efficiency (larger than 96%), and shorter operation times compared to original planning. Because of this low consumption, ASPOC continues to meet the Level 1 requirement, and the current level of operation can be maintained throughout the proposed extended mission.

6.3 Spacecraft system status

All four spacecraft are performing well, continue to meet requirements and far exceed the engineering design. There are no open subsystem or hardware risks. The primary consumable is hydrazine propellant, used to maintain orbit and attitude (Table 6.4). Delta-V analysis shows MMS can complete a

5-year extended mission with sufficient propellant reserve to meet the 25-year reentry requirement (predicted Earth reentry ~August 2030).

There have been few on-orbit anomalies to date. In February 2016 a suspected micrometeoroid impact damaged one of five parallel shunt resistors on the bottom deck of MMS4, which has not presented a concern. In March 2019 MMS1 Star Tracker camera head A exhibited voltage and temperature fluctuations requiring that head be turned off. There is no impact to navigation as there are 2 other functional camera heads and only one is required. Only 2 spacecraft processor resets have occurred (MMS4 in Jan. 2019 and MMS3 in June 2019).

The Mission Director tracks all risks using standard NASA risk management tools. The Continuous Risk Management (CRM) methodology is used to identify, analyze, plan, track, and control all risks. Operational mitigation techniques have been applied to maximize the likelihood that all four MMS observatories continue to operate reliably through the extended mission.

6.4 Mission operations status

The MMS Payload Operations Center (POC), located at LASP in Boulder, Colorado, operates the

Table 6.4: MMS Fuel Budget

Observatory	Current Fuel Masws (kg)	Orbit Formation/Maintenance/Eclipse (kg)	Available for Science Campaigns (kg)	Minimum Fuel Reserve EOM (2030) (kg)
MMS1	126.6	48	72.6	6
MMS2	122.3	48	68.3	6
MMS3	122.9	48	68.9	6
MMS4	123.3	48	69.3	6

MMS Instrument Suites in coordination with instrument teams. POC functions include routine planning and scheduling, command generation and uplink via the Mission Operations Center (MOC), health and safety assessment, contingency response, onboard and ground-based data management, and dissemination of data. The MOC at Goddard Space Flight Center (GSFC) performs all MMS spacecraft bus operations, including mission planning, real-time pass operations, systems and networks administration, IT security, observatory data trending, and systems engineering support.

All MMS telemetry are captured by the MOC and relayed, as they are received, to the POC using a high reliability private operational network. In addition to telemetry data transfers, ancillary data are provided to the POC via the MOC interface. The POC provides a real-time flow of data to the instrument teams to support commanding activities.

Onboard burst data management is a key function performed by the POC. Downlinked Fast Survey data are used to generate default burst data selections, which are made available to a Scientist-in-the-Loop (SITL) interface operated by the SDC and maintained by UCB. Designated scientists revise/improve the selections, which are submitted to the POC, processed, checked, and used to produce a revised downlink plan. The system maximizes the downlink of the highest value science data.

To reduce the operational burden of the mission, automated procedures for data selection are being tested. At present, there are three pathways for choosing which burst data segments are sent to the ground: 1) the SITL, 2) the on-board ABS (automatic burst selection), and 3) the GLS (ground loop system). The SITL examines the fast survey data to assign figures of merit (FOMs) to time intervals that fall in line with the SITL Guidelines. MMS is now fine tuning the ABS system with much improved selection of reconnection events. We are also testing the GLS system, which uses machine learning and a long-short-term memory recurrent neural network. This system is also showing very promising results. The plan is for the improved ABS and GLS systems to reduce greatly the load on the SITL within the next year. Results of these efforts are promising and will continue in the extended mission.

Starting in 2019 eclipse durations exceeding the design limit of 3.85 hours were unavoidable. The

MMS FDOA team performed extensive analysis to minimize eclipse durations via a 2019 apogee raise from 25 R_E to 29.34 R_E . While eclipses still exceed design they are significantly mitigated. Minimizing the risk of HV801 optocoupler delamination requires robust thermal and power analyses to ensure the instruments stay as warm as possible while the spacecraft also maintains positive battery power to prevent load shed. A custom set of operations for each eclipse season includes the power state (on, off, low power) of spacecraft subsystems and the Instrument Suite, the duration of heater operations, as well as a tilt of the instrument decks toward the Sun. All 4 observatories performed with no issues following two back-to-back 2019 extended eclipses with durations of 4:18 and 4:42, and all probes are well positioned for the next set of long duration eclipses. In summary, the current mission operations scenarios are well suited to meet the future needs of the MMS mission.

6.5 Publications

The scientific impact of MMS is demonstrated by its publication rates and citation statistics (Fig. 6.2): over 580 publications to date, more than 70 of which already have more than 40 citations.

A full list of MMS publications can be accessed at <https://lasp.colorado.edu/galaxy/x/p0e9Aw> with citation metrics constantly updating at <https://publons.com/researcher/2612056/>.

6.6 Communication and public outreach

Since 2015, the MMS Outreach team has participated in approximately 500 STEM conferences, public outreach events and programs, professional development trainings and meetings. We believe we have directly engaged more than 120,000 people in the MMS mission. MMS works in conjunction with NASA GSFC, and NASA HQ on efforts specifically focused to promote interest in NASA's endeavors and to foster participation in Science, Technology, Engineering, and Mathematics (STEM) fields. The site <https://lasp.colorado.edu/galaxy/x/w4BQ> contains relevant statistics for the first MMS extended mission. Other outreach efforts can be accessed at <https://mms.gsfc.nasa.gov/newsroom.html>.

6.7 Succession planning, training, and diversity

All key positions have deputies identified for the

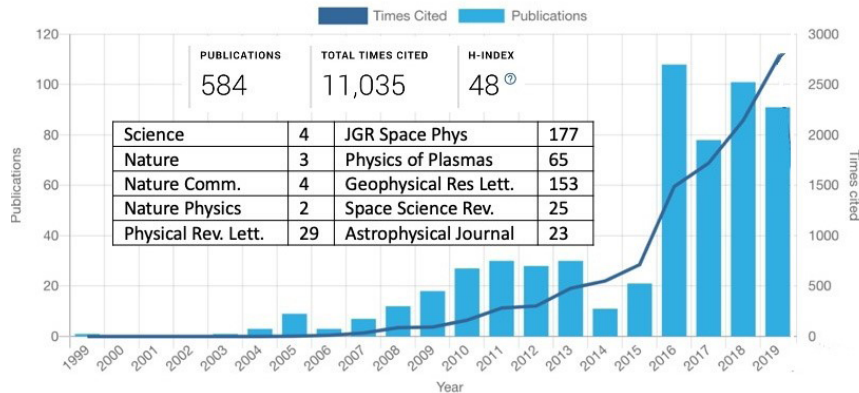


Fig. 6.2: MMS Publication statistics reveal the early impact of its theory/modeling program and, more recently, extensive utilization of the data by the world’s space and plasma physics communities.

We feel it is imperative to continue that program as it supports those exiting a postdoc position to establish a permanent position at the institution best suited to their development.

7 Data and Code Management

Maximum science output requires rapid access to quality science data products along with the tools to perform advanced analysis of those data sets. The team established, early on, a robust ground system to provide this service and is continually evolving that system as our instrument teams develop new products and tools.

purpose of succession planning and for training PIs and Project Scientists (Table 6.5). MMS continues to appoint new individuals to these career development positions in anticipation of their eventually assuming leadership positions on MMS or other missions. These deputies-in-training participate as ex-officio members of the MMS Science Working Group (SWG), which is the executive decision-making body for the broader MMS Science Working Team (SWT). A review of the current MMS organization structure (<https://lasp.colorado.edu/galaxy/x/WYAj>) shows both the depth and diversity of expertise able to meet requirements for every aspect of mission management.

ly on, a robust ground system to provide this service and is continually evolving that system as our instrument teams develop new products and tools.

MMS utilizes DSN, Space Network (SN), and Near Earth Network (NEN) via standard NASA services to provide ~5 DSN contacts every orbit (3.5 days) and 3 contacts spread across the SN and NEN. DSN contact time was recently renegotiated based on a 2019 loading study and an “as available and best effort” increase of ~8 hours per week has increased the daily downlink by an additional ~1 Gb of Science data per spacecraft (Fig. 7.1).

MMS has helped educate 14 new Ph.D. scientists, 10 Master-level graduates, and hundreds of science and engineering interns. Details can be accessed at <https://lasp.colorado.edu/galaxy/x/pUe9Aw>. In support of NASA HQ’s emphasis on increasing training and diversity, MMS supported two Early Career Scientist Grant programs, one in 2019 and one in 2020.

The MMS Science Data Center (SDC) (<https://lasp.colorado.edu/mms/sdc/public/>) serves as the central hub for MMS data related activities, including processing, archiving, visualization, and distribution. All Level-0 telemetry and Level-1 house-keeping are managed in a database system at the POC, which contains ~30 terabytes of data directly accessible to the instrument teams and FOT staff within 60 minutes of a contact. Over 99% of the data

collected onboard and requested for downlink has been successfully captured. Raw data from the Payload Operations Center (POC) are automatically ingested into the SDC and made available to the instrument teams along with ancillary data, for inspection, analysis, and processing to the higher-level data products.

MMS continues a vigorous calibration program to ensure the highest quality Level-2 products are available to the public within 30 days. Calibrations and corrections are continuously updated within each instrument complement and across instruments: they are mature

Table 6.5: Recent and Proposed MMS Leadership Trainees		
	Leaders in Training	Role
2018	Ian Cohen–JHU/APL	Deputy Lead–EPD
2019	Dan Gershman–GSFC	Deputy Lead–FPI
Proposed	Li-Jen Chen–NASA/GSFC	Deputy PS
Proposed	Kevin Genestreti–SwRI	Deputy PI
Proposed	Kyoung (Joo) Hwang–SwRI	Deputy PI
Proposed	James Webster–Rice	Deputy Lead–HPCA
Proposed	Matthew Argall–UNH	Deputy Lead–FIELDS
Proposed	Narges Ahmadi–LASP	Deputy Lead–ADP
Proposed	Rick Wilder–LASP	Deputy Lead–Burst Mode
Proposed	Yi-Hsin Liu–Dartmouth	Deputy Lead–T&M
Proposed	Christopher Riley–GSFC	Deputy SE Lead–MOC

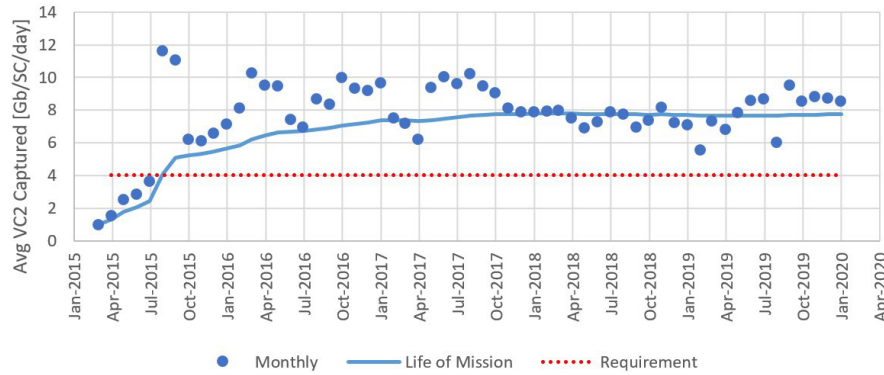


Fig. 7.1: Average VC2 Data Capture

and the products exceed Level-1 requirements. Cross-calibrations utilize independently computed parameters such as currents or densities (e.g., using FIELDS values of upper hybrid frequency to compare with FPI and HPCA densities), EPD/FPI/HPCA continuity of particle spectra, $V(e-i) \times B$ values compared to E , and others. This cross-calibration has greatly enhanced confidence in the data accuracies. Data User Guides continue to be expanded as teams further their calibrations and develop specialty analysis methodologies.

The SDC provides an array of public-access, web-based, data access tools supporting multiple platforms and methods. Interfaces are provided that can be used from a web browser, used on a command-line, or accessed via scripts or other software, and are intended for maximum versatility. There are also MMS data visualizations, including spacecraft in their orbit, the changing structure of the spacecraft formations, and auto-generated QuickLook data plots, which serve as a first glimpse of the returned data within ~ 24 hours. MMS data are stored in the Common Data Format (CDF) with full SPASE descriptions that were peer reviewed for maximum accessibility. All is fully documented via online guides linked to the front page of the public MMS SDC under the menu item “About the Data”. Each instrument’s data products page provides links to both a downloadable, searchable PDF document, and to a set of web page spreadsheets that fully enumerate and describe the data products available for each instrument in the CDF files.

All data within the SDC are continuously backed up both on-site and off-site to provide recovery in the case of system failure. The designated final archive for the MMS mission is the Space Physics Data Facility (SPDF), which also receives the MMS

Science products on an ongoing basis.

MMS collaborates with UCLA to provide data analysis tools through Space Physics Environment Data Analysis Software (SPEDAS), which facilitates direct access to all MMS data products and to analysis algorithms. SPEDAS is fully documented online (e.g., <http://spedas.org>),

and Python-based SPEDAS tools for MMS are now available. Training sessions and webinars on the use of SPEDAS with MMS data are regularly held at AGU meetings and MMS Community Data Analysis Workshops. A wide variety of other inexpensive or freeware software libraries (e.g., Autoplot) are also available.

As was required for MMS at launch, a Project Data Management Plan (PDMP) was developed and approved by the Heliophysics Division at NASA HQ. The archival data products are fully described in the PDMP, which is proposed to be updated and approved by the end of FY21. Initial edits to the PDMP are reflected in Appendix C; final edits by the instrument teams were delayed by the Spring 2020 COVID-19 outbreak. The work will be completed, and no further resources are anticipated for this update.

MMS did not have a previous requirement for a Calibration and Measurement Algorithms Document (CMAD) and so began development on receipt of the Call for Proposals. Fortunately, the MMS teams have been diligent about documenting these items in both peer review publications and in the Data User Guides available at the MMS SDC website. The CMAD is proposed to be completed and approved by the end of FY21. An outline of the content is included as Appendix D; further work was delayed by the Spring 2020 COVID-19 outbreak. The work will be completed, and no further resources are anticipated for this development.

All mission documents and project-originated processing and analysis codes key to utilizing the science data will be referenced in the PDMP and CMAD and, as appropriate, will be archived in the documents directories within the mission section of the SPDF heliophysics archives. A SPASE <http://>

spase-group.org> document resource will be created to point to each document and a DOI will be assigned that will lead to a landing page for the document. Similarly, MMS intends to partner with the SPDF for implementation of all open-source requirements. MMS is fully committed to the policies concerning open access to data as outlined under OMB memo M-13-13, as well as the ‘NASA Plan for Increasing Access to the Results of Scientific Research’ and the Heliophysics Data Policy.

8 Budget Justification

MMS is managed by GSFC, as the Project Management and Mission Operations organization, and Southwest Research Institute (SwRI) for Payload and Science Management. GSFC project management includes administration and reporting, Science operations coordination, budgeting, contract and grant administration, mission operations, and a minimal Science component. SwRI is under contract to GSFC and leads the Solving Magnetospheric Acceleration, Reconnection, and Turbulence (SMART) Science investigation. This work includes Science research and publication, Science and payload operations, theory and modeling, data processing and analysis, data archiving and community Science support. Throughout its operations, MMS spending has been kept well within the funding appropriations and has been carefully managed. No changes are planned to the management structure in the extended mission.

Two budget spreadsheets are attached. The first spreadsheet details an in-guideline MMS budget covering fiscal years 2021-2025; the second details an over-guideline budget for the same period. The in-guide budget results in only tetrahedron formations, and curtailment of science investigations not directly related to reconnection physics. Approximately ~40 scientists and engineers lose their funding with the in-guide budget by 2023. The proposed over-guideline budget supports the proposed payload and mission operations and scientific research through FY25, while reducing the annual operations costs as recommended by the 2017 Senior Review. Neither budget includes a final closeout year.

The proposed over-guideline budget gradually ramps down yearly by ~10% per year until settling on a constant baseline budget of \$16.8M in FY25.

MMS-SMART Budget. SMART funding supports

project activities at SwRI and several subcontractor institutions as well as government contributions (FPI at GSFC/MSFC and EPD at LANL) that are overseen by SwRI. Several efforts – including T&M, MEC, early career, and SITL – are administered by the PS office to minimize overhead.

The overguide budget supports continued operations and scientific research at levels comparable to, but somewhat lower than those of the highly successful prime phase and first extended mission. It continues to deliver unique measurements and new analyses to realize the full promise of the mission. With its four spacecraft and 100 instruments, which enable a temporal and spatial resolution far exceeding that ever before achieved in space, MMS is a high-precision laboratory instrument of heretofore unimaginable capabilities. Wise use of fuel reserves render it essential to optimize scientific return enabled by the use of both the usual tetrahedron formation, an opportunity that will not occur again in any mission for the foreseeable future, and new configurations that enable new science. Experience shows that fine-tuning of the MMS “microscope” must be guided by the most recent scientific progress leading to tailored configurations for investigations of different phenomena. Neither routine operations nor completely automated algorithms can serve as substitutes, although the team is implementing automated algorithms to reduce the operational burden whenever possible.

Budget for GSFC Management and Mission Operations. MMS funding has supported activities at GSFC within the Heliophysics Science Division (HSD), at two IDS PI Institutions, the Space Sciences Mission Operations (SSMO) Project office, and the Mission Validation and Operations Branch, including contracted services. During the last extended mission phase, Project Science and SSMO funding accounts for ~28% of the total mission budget as is roughly preserved in the proposed budget. We are proposing extended mission operations based on experience with MMS tetrahedron formation flying operations during Phase E and the present extended mission. These operations were very challenging in terms of the number and frequency of maneuvers required to maintain the four spacecraft in scientifically optimal orbits. Nevertheless, the SSMO team was able to operate the spacecraft with mean separations as close as 7 km in Phase E, which proved essential

to resolve electron physics of reconnection. MMS flies in tetrahedron formation at least through FY 2023, but with somewhat larger minimum separations (~20 km) owing to its higher apogee. After this period, if operating with the over-guide budget, new configurations as described in §5 are implemented. An estimate of required High End Computing Resources is included to support the state-of-the-art kinetic modeling proposed, in close association with MMS measurements.

9 References

- Bandyopadhyay, R., et al. (2018), *ApJ*, 866, 2, [doi:10.3847/1538-4357/AADE93](https://doi.org/10.3847/1538-4357/AADE93)
- Breuillard, H. et al. (2018), *ApJ*, 859,127, [doi:10.3847/1538-4357/aabae8](https://doi.org/10.3847/1538-4357/aabae8)
- Burch, J. L. et al. (2018a), *GRL*, 45,1237–1245, [doi:10.1002/2017GL076809](https://doi.org/10.1002/2017GL076809)
- Burch, J. L., et al. (2018b), *JGR*, 123, 2, [doi:10.1002/2017JA024789](https://doi.org/10.1002/2017JA024789)
- Burch, J. L., et al. (2019), *GRL*, 46, 8, [doi:10.1029/2019GL082471](https://doi.org/10.1029/2019GL082471)
- Chasapis, A. et al. (2017), *ApJL*, 844, 1, [doi:10.3847/2041-8213/AA7DDD](https://doi.org/10.3847/2041-8213/AA7DDD)
- Chasapis, A. et al. (2018), *ApJ*, 862, 1, [doi:10.3847/1538-4357/AAC775](https://doi.org/10.3847/1538-4357/AAC775)
- Cohen, I. J. et al. (2019), *GRL*, 46, [doi:10.1029/2019GL082008](https://doi.org/10.1029/2019GL082008)
- Dokgo, K., et al. (2019), *GRL*, 46, 14, [doi:10.1029/2019GL083361](https://doi.org/10.1029/2019GL083361)
- Eastwood, J. P. et al. (2018), *GRL*, 45, 4569–4577, [doi:10.1029/2018GL077670](https://doi.org/10.1029/2018GL077670)
- Engebretson, M. J., et al. (2018), *JGR*, 123, [doi:10.1029/2018JA025984](https://doi.org/10.1029/2018JA025984)
- Ergun, R. E., et al. (2017), *GRL*, 44, 2978–2986, [doi:10.1002/2016GL072493](https://doi.org/10.1002/2016GL072493)
- Ergun, R. E. et al. (2018), *GRL*, 45, 3338–3347, [doi:10.1002/2018GL076993](https://doi.org/10.1002/2018GL076993)
- Fox, W. et al. (2018), *GRL*, 45, 23, [doi:10.1029/2018GL079883](https://doi.org/10.1029/2018GL079883)
- Fuselier, S. A. et al. (2019), *GRL*, 46, 6204–6213, [doi:10.1029/2019GL082384](https://doi.org/10.1029/2019GL082384)
- Genestreti, K. J. et al. (2018), *JGR*, 123, 1806–1821, [doi:10.1002/2017JA025019](https://doi.org/10.1002/2017JA025019)
- Gingell, I. et al. (2019), *GRL*, 46, 1177–1184, [doi:10.1029/2018GL081804](https://doi.org/10.1029/2018GL081804)
- Graham, D. B., et al. (2018), *JGR*, 123(4):2630–2657, [doi:10.1002/2017JA025034](https://doi.org/10.1002/2017JA025034)
- Graham, D. B. et al. (2019). *JGR*, 124, [doi:10.1029/2019JA027155](https://doi.org/10.1029/2019JA027155)
- Johlander, A. et al. (2018), *Plasma Physics and Controlled Fusion*, 60,12, [doi:10.1088/1361-6587/AAE920](https://doi.org/10.1088/1361-6587/AAE920)
- Kitamura, N. et al. (2018), *Science*, 361, 6406, [doi:10.1126/Science.AAP8730](https://doi.org/10.1126/Science.AAP8730)
- Le, A. et al. (2018), *PhPl*, 25, 6, [doi:10.1063/1.5027086](https://doi.org/10.1063/1.5027086)
- Lichko, E. et al. (2020), *Nature Comm.*, in press.
- Lu, S. W., et al. (2019), *ApJ*, [doi:10.3847/1538-4357-ab0e76](https://doi.org/10.3847/1538-4357-ab0e76)
- Marshall, A. T. et al. (2019), *JGR*, 125, [doi:10.1029/2019JA027296](https://doi.org/10.1029/2019JA027296)
- Nakamura, R. et al. (2019), *JGR*, 124, 1173–1186, [doi:10.1029/2018JA026028](https://doi.org/10.1029/2018JA026028)
- Nykyri, K. et al. (2019), *JGR*, 124, 197–210, <https://doi.org/10.1029/2018JA026131>
- Øieroset, M. et al. (2019), *GRL*, 46, 1937–1946, [doi:10.1029/2018GL080994](https://doi.org/10.1029/2018GL080994)
- Oimatsu, S., et al. (2018), *GRL*, 45, [doi:10.1029/2018GL078961](https://doi.org/10.1029/2018GL078961)
- Oka, M. et al. (2019), *ApJ*, 866, 1, [doi:10.3847/1538-4357/ab4a81](https://doi.org/10.3847/1538-4357/ab4a81)
- Phan, T. D. et al. (2018), *Nature*. 557, [doi:10.1038/s41586-018-0091-5](https://doi.org/10.1038/s41586-018-0091-5)
- Swisdak, M. et al. (2018), 45, 5260–5267, *GRL*, [doi:10.1029/2017GL076862](https://doi.org/10.1029/2017GL076862)
- Stawarz, J. et al. (2019), *ApJL*, 877, 2, [doi:10.3847/2041-8213/ab21c8](https://doi.org/10.3847/2041-8213/ab21c8)
- Toledo-Redondo, S. et al. (2018), *GRL*, 45, 10,033, [doi:10.1029/2018GL079051](https://doi.org/10.1029/2018GL079051)
- Torbert, R. B. et al. (2018), *Science*, 362, 6421, [doi:10.1126/Science.aat2998](https://doi.org/10.1126/Science.aat2998)
- Turner, D. L. et al. (2017), *JGR*,122,11,481–11,504, [doi:10.1002/2017JA024554](https://doi.org/10.1002/2017JA024554)
- Turner, D. L. et al. (2018), *Nature*, 561, 206-210, [doi:10.1038/S41586-018-0472-9](https://doi.org/10.1038/S41586-018-0472-9)
- Vines, S. K. et al. (2019), *GRL*, 46, 5707–5716, [doi:10.1029/2019GL082152](https://doi.org/10.1029/2019GL082152)
- Wang, S. et al. (2019), *GRL*, 46, 562–570, [doi:10.1029/2018GL080944](https://doi.org/10.1029/2018GL080944)
- Webster, J. M. et al. (2018), *JGR*, 123, 4858–4878, [doi:10.1029/2018JA025245](https://doi.org/10.1029/2018JA025245)
- Wilder, F. D. et al. (2018), *JGR*, 123, 6533–6547, [doi:10.1029/2018JA025529](https://doi.org/10.1029/2018JA025529)

Appendix A: MMS Acronym List

Acronym	Definition
ABS	Automatic Burst Selection
AC	Alternating Current
ACE	Advanced Composition Explorer
AEM	Ambient Electron Mode
AFG	Analog Flux Gate
AI	Artificial Intelligence
ARTEMIS	Acceleration, Reconnection, Turbulence and Electrodynamics of the Moon's Interaction with the Sun
ASCII	American Standard Code for Information Interchange
ASPOC	Active Spacecraft Potential Control
AU	Astronomical Unit
CDF	Common Data Format
CIR	Corotating Interaction Region
CMAD	Calibration and Measurement Algorithms Document
CPS	Central Plasma Sheet
CRM	Continuous Risk Management
DC	Direct Current
DES	Dual Electron Sensor
DF	Dipolarization Front
DFG	Digital Fluxgate
DIS	Dual Ion Sensor
DL	Double Layer
DMC	Diamagnetic Cavity
DSA	Diffusive Shock Acceleration
DSCOVR	Deep Space Climate Observatory
DSN	Deep Space Network
EDI	Electron Drift Instrument
EDR	Electron Diffusion Region
EIS	Energetic Ion Spectrometer
EMIC	Electromagnetic Ion Cyclotron
EOM	End of Mission
EPD	Energetic Particle Detectors
ERG	Exploration of Energization and Radiation in Geospace
ESW	Electrostatic Waves
FB	Foreshock Bubble
FDOA	Flight Dynamics Operations Area
FEEPS	Fly's Eye Energetic Particle Spectrometer
FIELDS	MMS suite of electric and magnetic field instruments
FOT	Flight Operations Team
FOM	Figures of Merit
FPI	Fast Plasma Instrument
FTE	Flux Transfer Event
FY	Fiscal Year
GOES	Geostationary Operational Environmental Satellite
GLS	Ground Loop System
GSE	Geocentric Solar Ecliptic

Acronym	Definition
GSFC	Goddard Space Flight Center
GSM	Geocentric Solar Magnetospheric
HFA	Hot Flow Anomaly
HPCA	Hot Plasma Composition Analyzer
HSD	Heliophysics Science Division
HSO	Heliophysics System Observatory
HV	High Voltage
IBEX	Interstellar Boundary Explorer
IMAP	Interstellar Mapping and Acceleration Probe
IMF	Interplanetary Magnetic Field
IP	Interplanetary
JAXA	Japan Aerospace Exploration Agency
KH	Kelvin-Helmholtz
LANL	Los Alamos National Laboratory
LASP	Laboratory for Atmospheric and Space Physics
LEO	Low Earth Orbit
LHW	Lower-Hybrid Waves
LMN	Boundary Normal Coordinates
LT	Local Time
MCP	Microchannel Plate
MEC	Magnetic Ephemeris Coordinates
MHD	Magnetohydrodynamics
MLT	Magnetic Local Time
MMS	Magnetospheric Multiscale Mission
MOC	Mission Operations Center
MSFC	Marshall Space Flight Center
N/A	Not Applicable
NASA	National Aeronautics and Space Administration
NEN	Near Earth Network
NISM	Near Interstellar Medium
OMB	Office of Management and Budget
P&SS	Planetary and Space Science
PDF	Portable Document Format
PDMP	Project Data Management Plan
PI	Principal Investigator
POC	Payload Operations Center
PS	Project Scientist
PSBL	Plasma Sheet Boundary Layer
PSG	Prioritized Science Goal
PSP	Parker Solar Probe
PUI	Pickup Ion
R_E	Earth Radii
RF	Radio Frequency
ROI	Regions of Interest
S/C	Spacecraft
SCM	Search Coil Magnetometer
SDA	Shock Drift Acceleration
SDC	Science Data Center

Acronym	Definition
SDP	Spin-plane Double Probe
SITL	Scientist-in-the-Loop
SLAM	Short Large Amplitude Magnetic structure
SMART	Solving Magnetospheric Acceleration, Reconnection, and Turbulence
SMD	Science Mission Directorate
SN	Space Network
SO	Science Objective
SOC	Science Operations Center
SOHO	Solar and Heliospheric Observatory
SPASE	Space Physics Archive Search and Extract
SPDF	Space Physics Data Facility
SPEDAS	Space Physics Environment Data Analysis Software
SR	Science Review
SROI	Science Regions of Interest
SSCWeb	Satellite Situation Center Web
SSMO	Space Sciences Mission Operations
STEM	Science, Technology, Engineering and Mathematics
SW	Solar Wind
SWG	Science working group
SwRI	Southwest Research Institute
SWT	Science Working Team
T&M	Theory and Modeling
THEMIS	Time History of Events and Macroscale Interactions during Substorms mission
UCB	University of California – Berkeley
UCLA	University of California – Los Angeles
ULF	Ultra-Low Frequency
USAF	United States Air Force
VAP	Van Allen Probes
VDF	Velocity Distribution Function
XML	Extensible Markup Language

Appendix B: Code 300 Evaluation of End of Mission Plan

370

May 26, 2020

TO: 300/Director, Safety & Mission Assurance Directorate
FROM: 370/Quality & Reliability Division/Viens
SUBJECT: Code 300 Evaluation of End of Mission Plan for Magnetospheric Multiscale Mission
REF: a) NASA-STD-8719.14B, Process for Limiting Orbital Debris
b) Call for Proposals, Rev 2b — Senior Review 2020 of the Mission Operations and Data Analysis Program for the Heliophysics operating missions, Revision 2b: February 7, 2020. NASA HQ / N. Fox / Director, Heliophysics Division, NASA HQ / J. Leisner / Senior Review, Program Scientist, NASA HQ / Heather Futrell (W. Stabnow retired effective May 2020) / Senior Review, Program Executive
c) Magnetospheric Multiscale End of Mission Plan, SSMO-MMS-EOMP-0011, dtd February 2020

The Magnetospheric Multiscale (MMS) mission has demonstrated full compliance with NASA-STD-8719.14B in an End of Mission Plan (EOMP), dated February 2020. The EOMP was developed using a baseline end of mission date of October 1, 2023, though the mission will continue to be in compliance if continued beyond that date. MMS consists of a constellation of four spacecraft in highly eccentric orbits with perigee of ~1500 km, apogee of ~187,500 km, and 14.6° inclination. Disposal is intended by adjusting the orbit to result in uncontrolled reentry in 2030. The probes will be passivated to the extent possible prior to the orbit decay period. ORSAT assessment indicates that the probes will fully demise on reentry due to the high eccentricity orbit.

As there is an existing EOMP, no additional EOMP analysis is required. Further details are documented in the EOMP, available from the SSMO Configuration Management Office. Please feel free to contact me (301-286-2505), if you have any questions or concerns.

Michael Viens

Michael Viens

Cc: 370/Nowak, Sticka, JIRA,
380/Maggio
300/Leitner
592/Hull
HQ-SMD/H. Futrell
SSMO/R. Burns